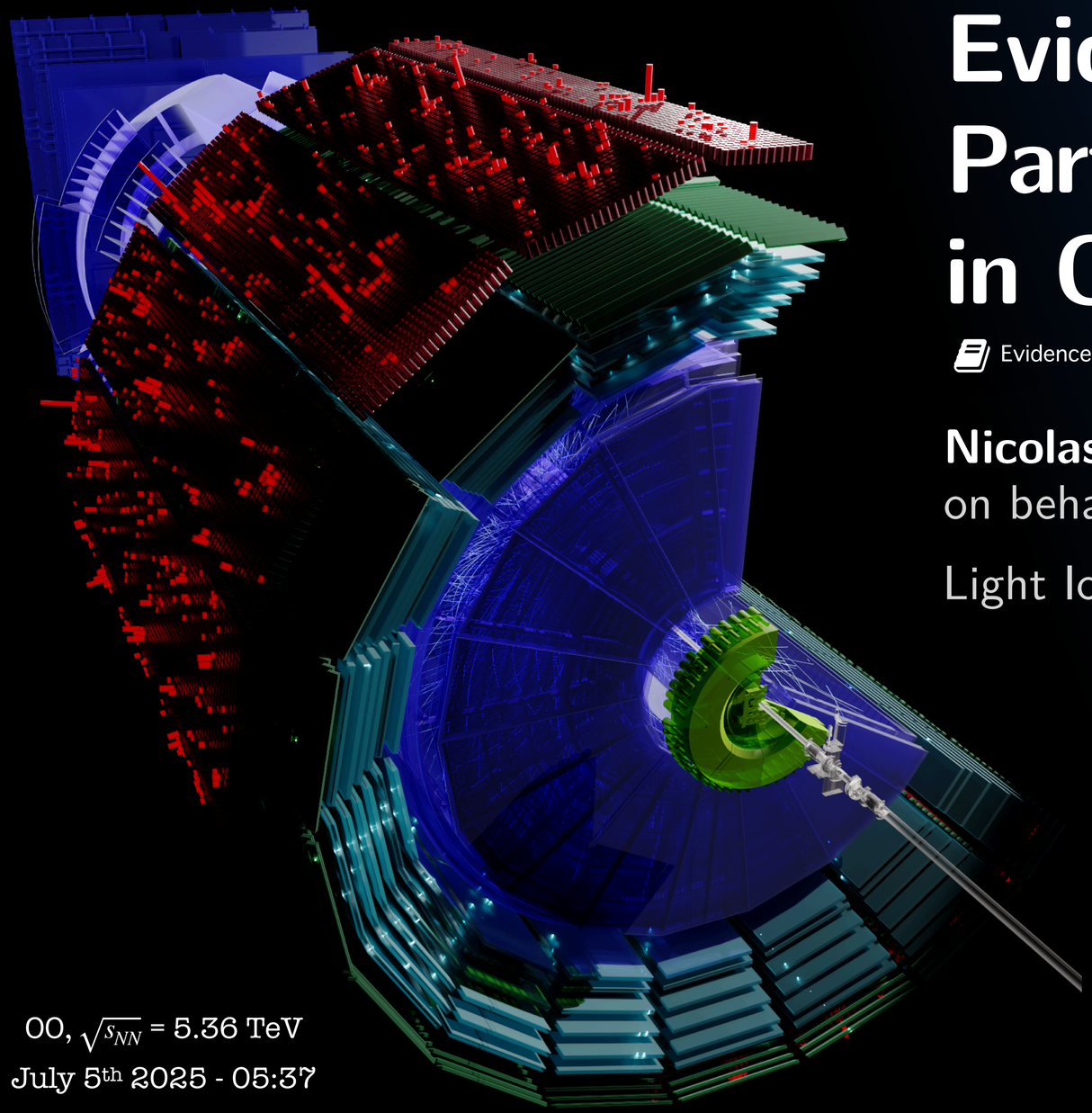


OO, $\sqrt{s_{NN}}$ = 5.36 TeV
July 5th 2025 - 05:37

Evidence for Parton Energy Loss in OO Collisions with ALICE

Evidence for parton energy loss in OO: arXiv:2606.19967

Supplemental material: ALICE-PUBLIC-2026-002

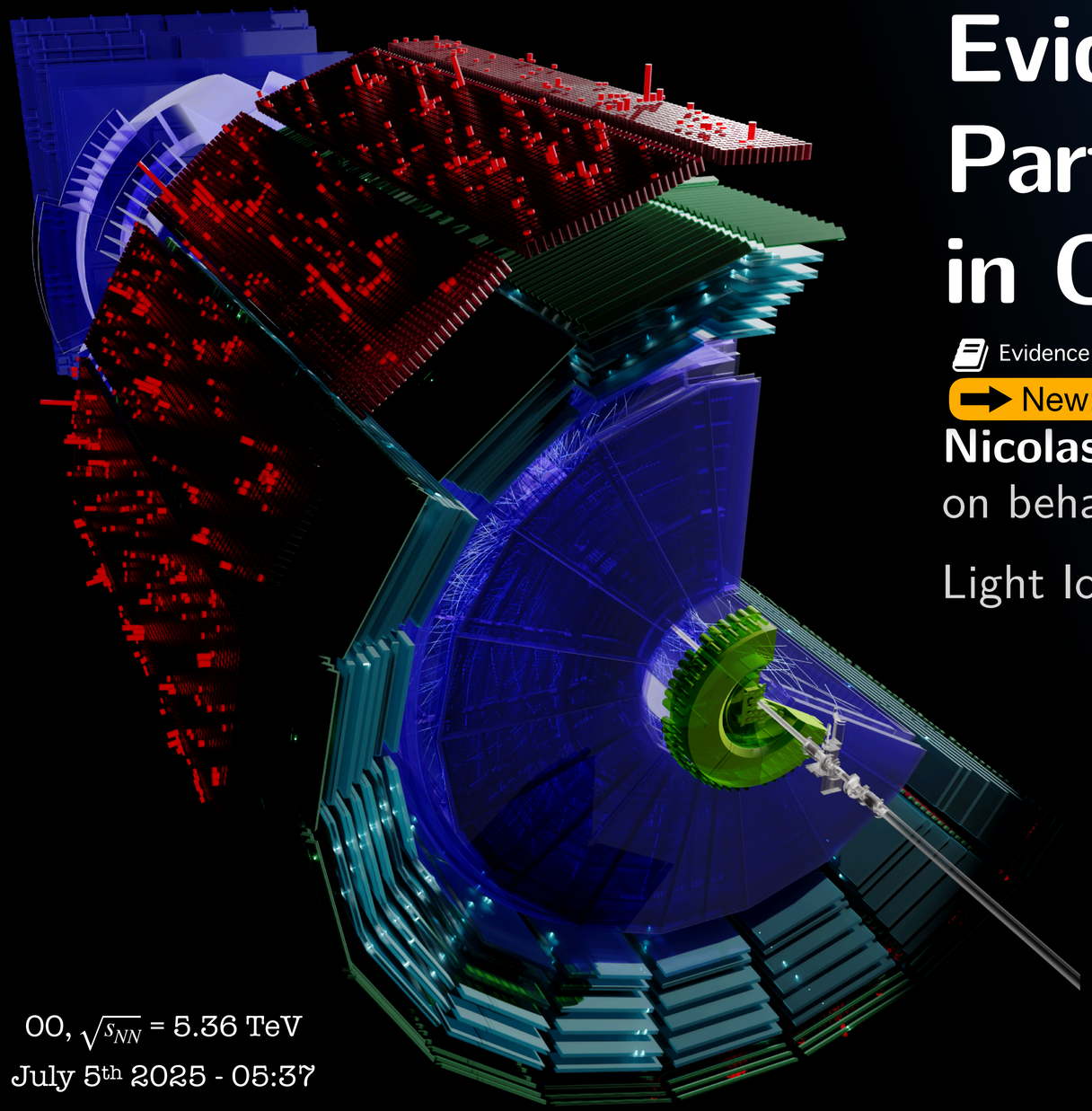
Nicolas Strangmann
on behalf of the ALICE collaboration

Light Ion Workshop, Heidelberg, 22. September 2026

HGS-HIRe for FAIR
Helmholtz Graduate School for Hadron and Ion Research

FSP ALICE
Erforschung von Universum und Materie

GOETHE UNIVERSITÄT FRANKFURT AM MAIN



OO, $\sqrt{s_{NN}}$ = 5.36 TeV
July 5th 2025 - 05:37

Evidence for Parton Energy Loss in OO Collisions with ALICE

Evidence for parton energy loss in OO: arXiv:2606.19967

Supplemental material: ALICE-PUBLIC-2026-002

New: Accepted by PRL

Nicolas Strangmann
on behalf of the ALICE collaboration

Light Ion Workshop, Heidelberg, 22. September 2026

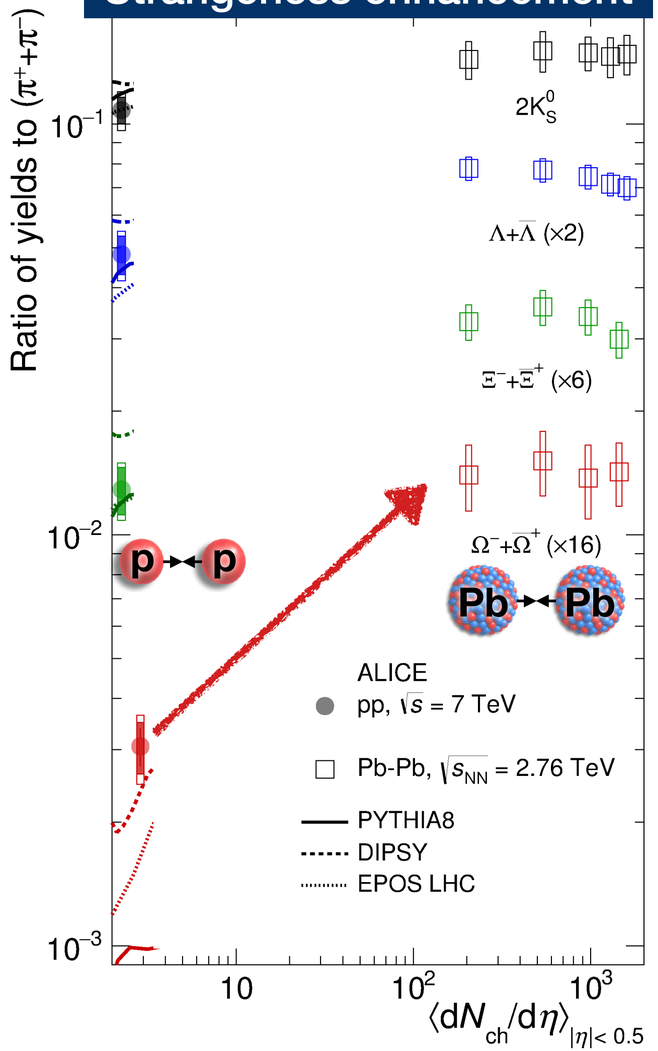
HGS-HIRe for FAIR
Helmholtz Graduate School for Hadron and Ion Research

FSP ALICE
Erforschung von Universum und Materie

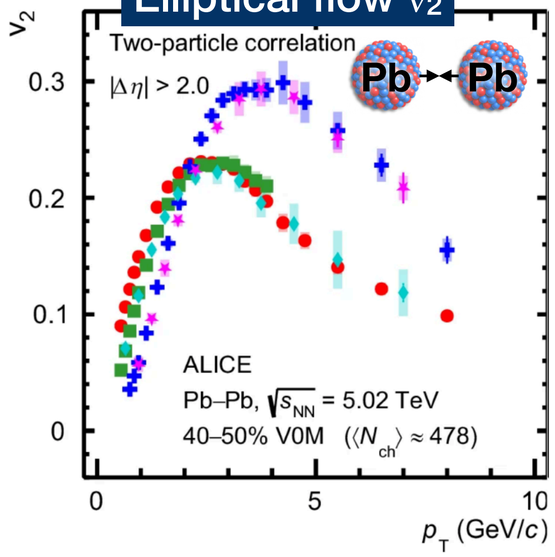
GOETHE UNIVERSITÄT FRANKFURT AM MAIN

QGP Signatures in Small Systems

Strangeness enhancement



Elliptical flow v_2

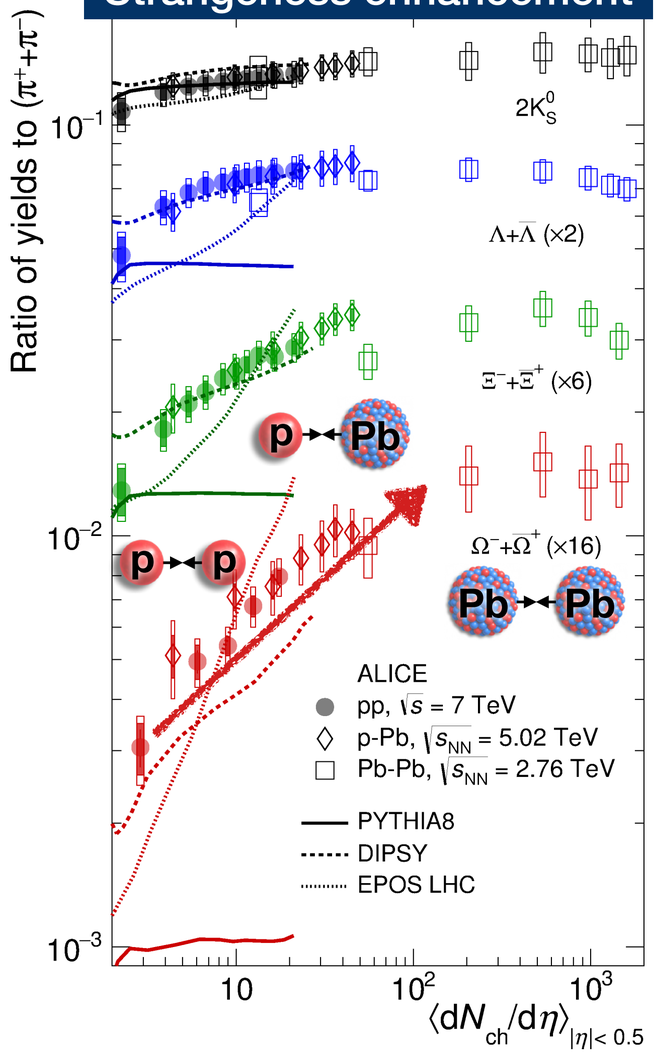


Strangeness enhancement: ALICE, Nat. Phys. 13 (2017) 535-539

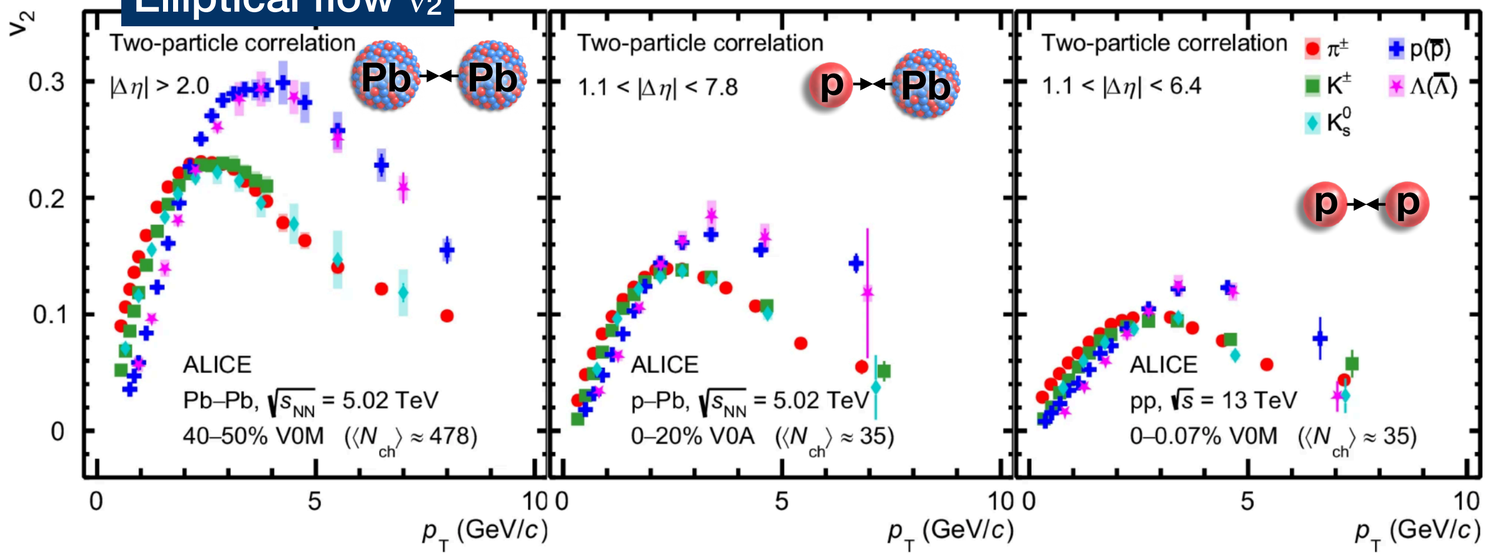
Elliptical flow: ALICE, Nat. Commun. 17 (2026) 1, 2585

QGP Signatures in Small Systems

Strangeness enhancement



Elliptical flow v_2



Several features attributed to the QGP observed in high-multiplicity pp and p—Pb collisions at the LHC

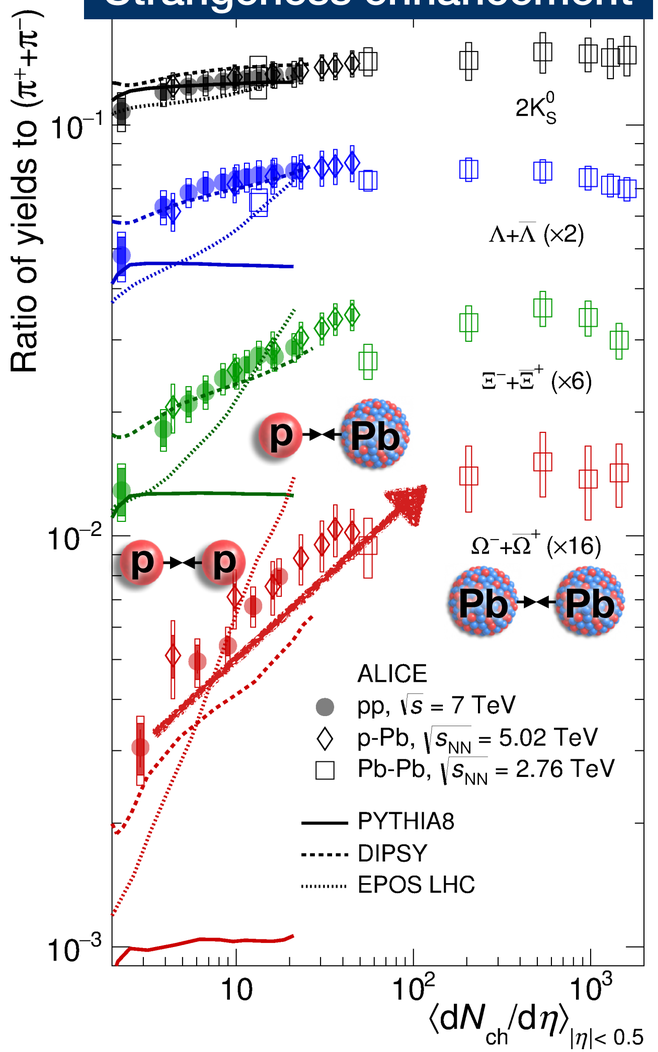
→ Challenging traditional assumptions of small systems as “QGP-free” references for Pb—Pb

Strangeness enhancement: ALICE, Nat. Phys. 13 (2017) 535-539

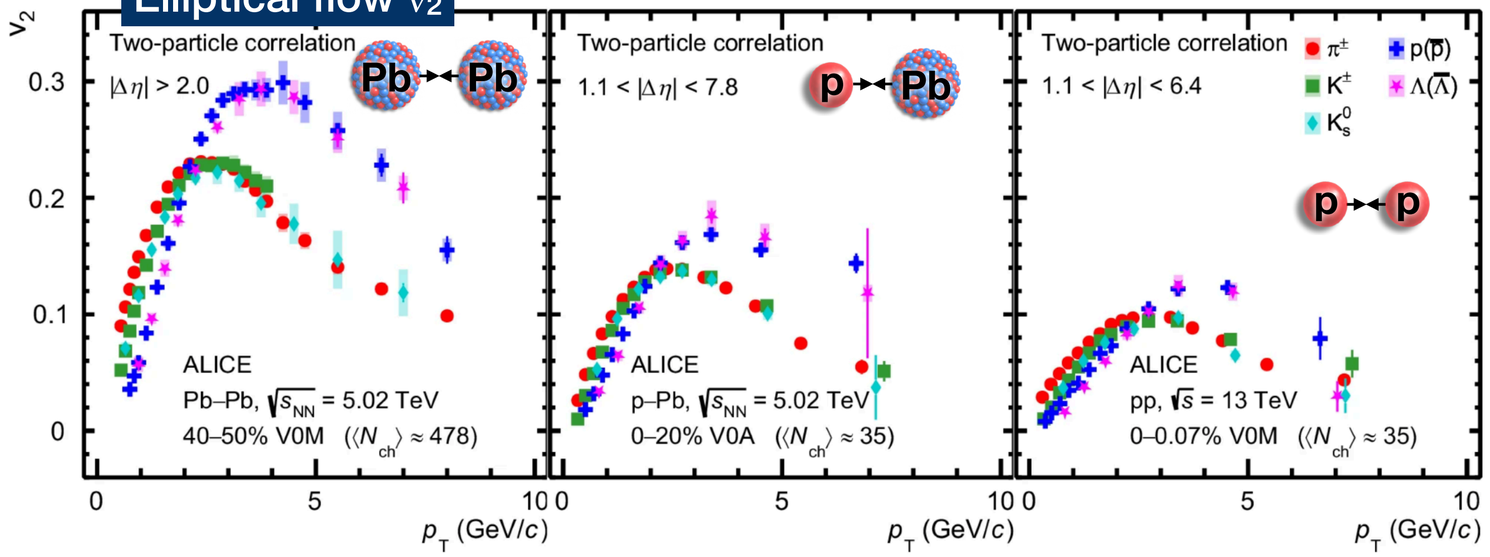
Elliptical flow: ALICE, Nat. Commun. 17 (2026) 1, 2585

QGP Signatures in Small Systems

Strangeness enhancement



Elliptical flow v_2



Several features attributed to the QGP observed in high-multiplicity pp and p—Pb collisions at the LHC

→ Challenging traditional assumptions of small systems as "QGP-free" references for Pb—Pb

BUT no observation of parton energy loss in pp or p—Pb

Strangeness enhancement: ALICE, Nat. Phys. 13 (2017) 535-539

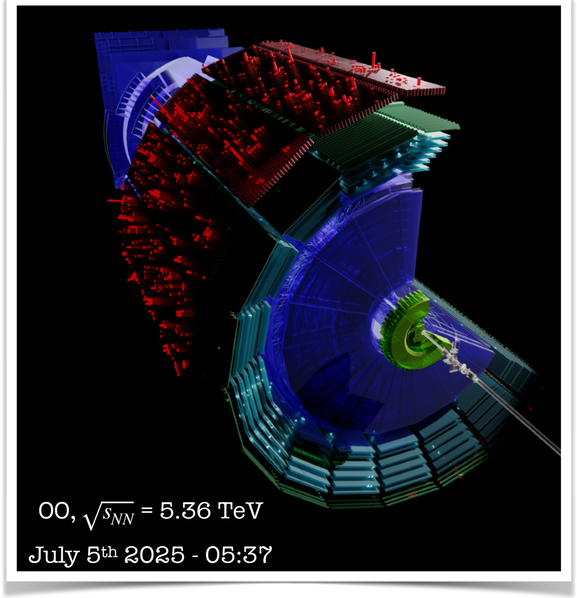
Elliptical flow: ALICE, Nat. Commun. 17 (2026) 1, 2585

Light Ions Data Taking — July 2025

- **Outstanding LHC performance**
  - 37h of stable OO beams over 7 fills
    → 5 nb^{-1} recorded luminosity (expectation was 0.5 nb^{-1})
- Excellent detector stability throughout the campaign
- Sparse filling scheme in OO (40 interacting bunches)
  → Up to μ = 0.1 (5% pile-up correction in OO analysis)

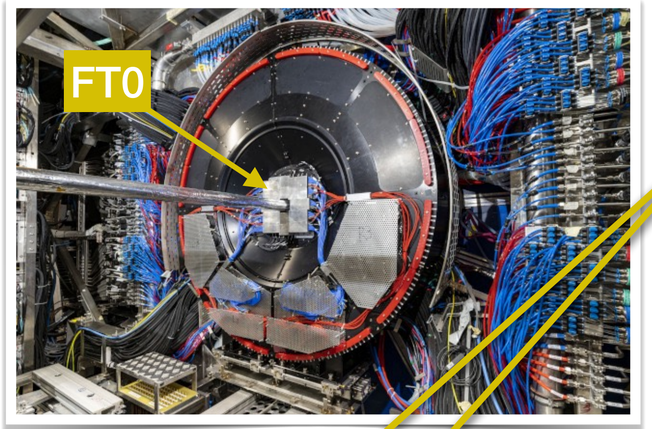


	p–O	O–O	p–p	p–p
$\sqrt{s_{NN}}$	9.62 TeV	5.36 TeV	5.36 TeV	13.6 TeV
Data taking	2025	2025	2024	2023
Rate	15 kHz	35 kHz	~1 MHz	~500 kHz
μ	0.04	0.09	0.033	0.025
$\mathcal{L}_{int}^{rec}$	7.3 nb^{-1}	5.0 nb^{-1}	5.3 pb^{-1}	9.7 pb^{-1}

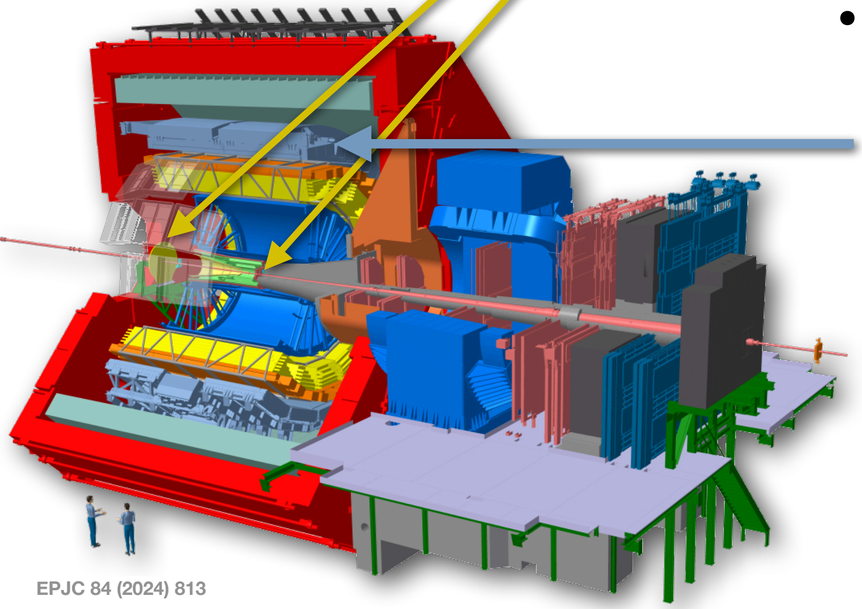


Detector Setup

ALICE received major upgrades during LS2, including FIT



Wladyslaw Henryk Trzaska



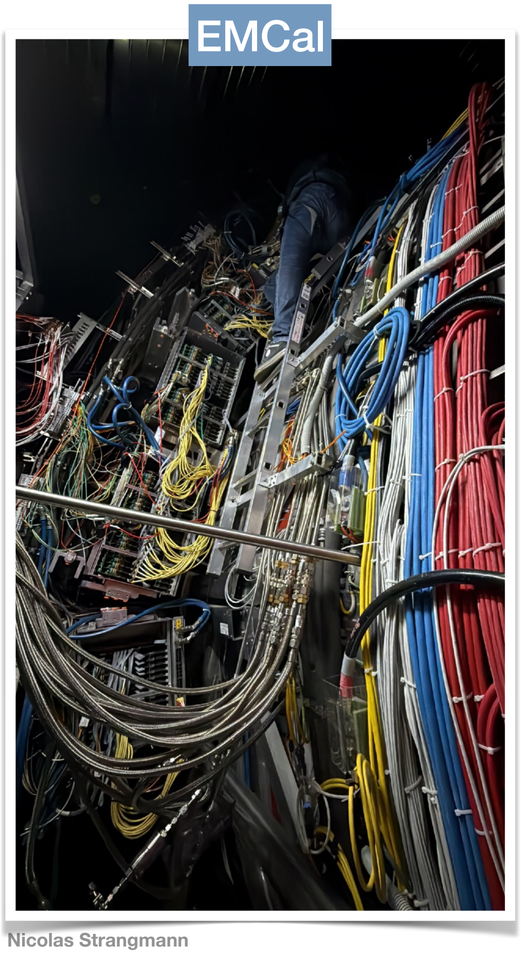
EPJC 84 (2024) 813

Fast Interaction Trigger (FIT)

- Includes two Cherenkov arrays (FT0) on either side of the interaction point
- Triggers on coincident signal
- Used to determine/restrict vertex z position
- Covers $-3.3 < \eta < -2.1$ & $3.5 < \eta < 4.9$

ElectroMagnetic Calorimeter (EMCal)

- Lead-scintillator calorimeter
- Refurbished readout and enabled multi-event buffering
- Photon reconstruction for $E_\gamma \gtrsim 600$ MeV
- Photon identification using shower shape



Nicolas Strangmann

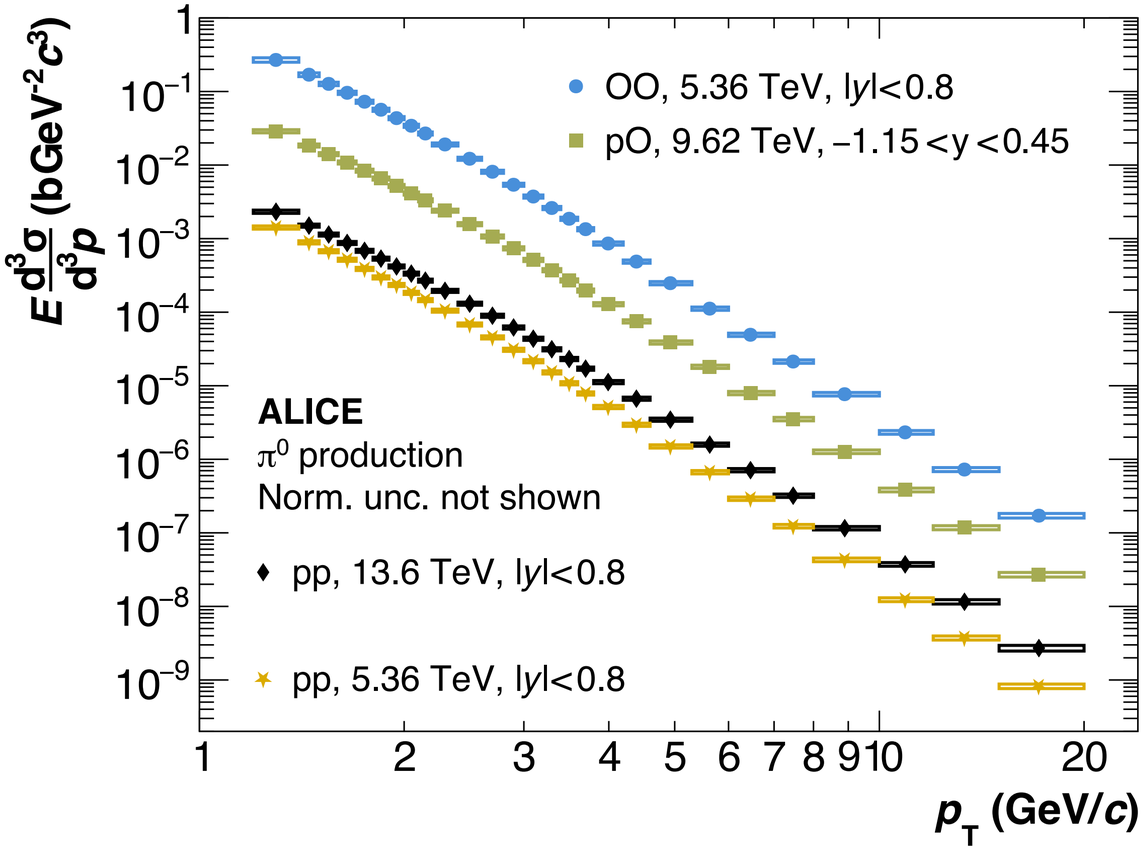
π^0 Production Cross Sections

Measurement of π^0 production in

- **OO** (5.36 TeV), **pO** (9.62 TeV), **pp** (13.6 TeV) and **pp** (5.36 TeV)
- 1.2 GeV/c < p_T < 20 GeV/c, $|y_{lab}| < 0.8$
- Statistical uncertainty $\lesssim$ 1% at intermediate p_T
- Systematic uncertainty ~6%
  (4.2% from material budget → cancels in ratios)

Normalization uncertainties

OO, 5.36 TeV: 2%
pO, 9.62 TeV: 2.7%
pp, 13.6 TeV: 2.6%
pp, 5.36 TeV: 2.6%



π^0 Production Cross Sections

Measurement of π^0 production in

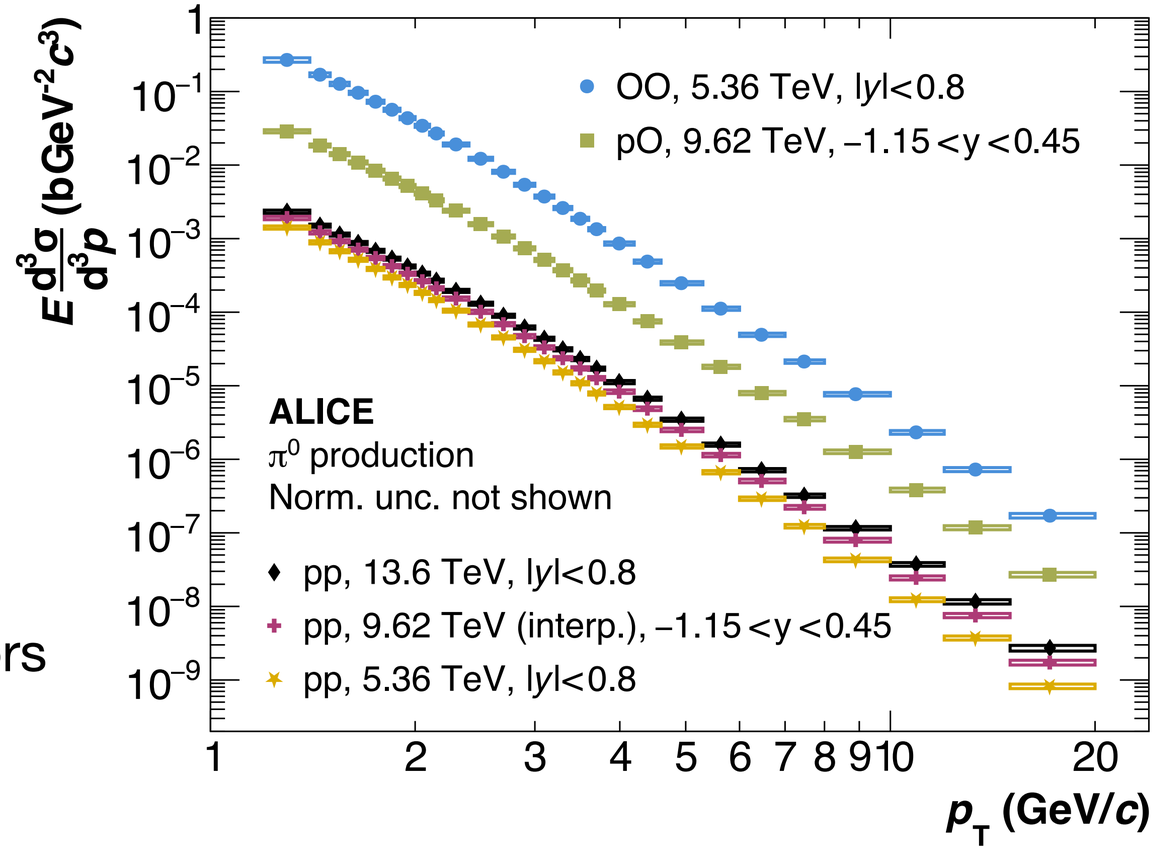
- **OO** (5.36 TeV), **pO** (9.62 TeV), **pp** (13.6 TeV) and **pp** (5.36 TeV)
- 1.2 GeV/c < p_T < 20 GeV/c, $|y_{lab}| < 0.8$
- Statistical uncertainty $\lesssim$ 1% at intermediate p_T
- Systematic uncertainty ~6%
  (4.2% from material budget → cancels in ratios)

Normalization uncertainties

OO, 5.36 TeV: 2%
pO, 9.62 TeV: 2.7%
pp, 13.6 TeV: 2.6%
pp, 5.36 TeV: 2.6%

Interpolation to pp (9.62 TeV)

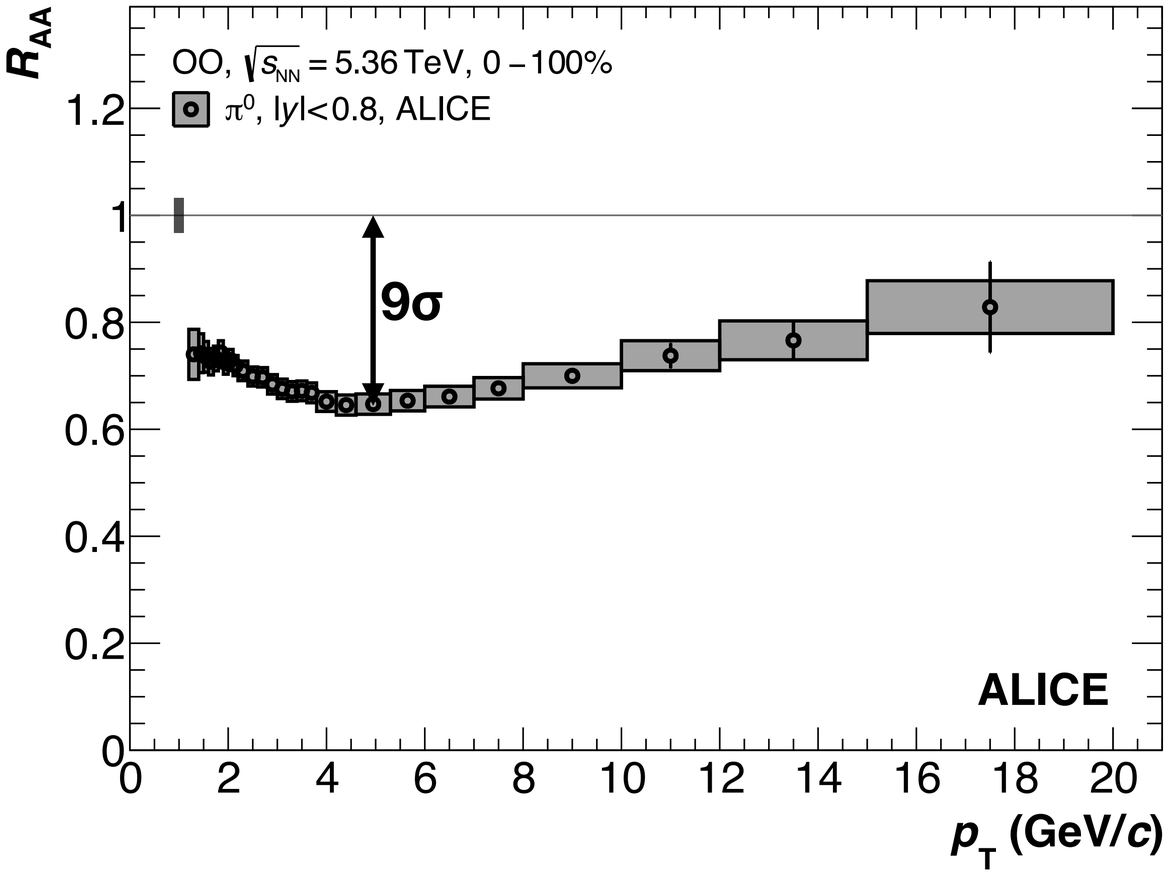
- Required as reference for pO
- Interpolation between pp at 5.36 and 13.6 TeV
- Using three independent $\sqrt{s}$ dependence estimators
- Rapidity shift based on PHYTHIA8 (<1%)



Nuclear Modification of π^0 Production: R_{OO}

$$R_{AA} = \frac{1}{A^2}\frac{\sigma_{AA}}{\sigma_{pp}}$$

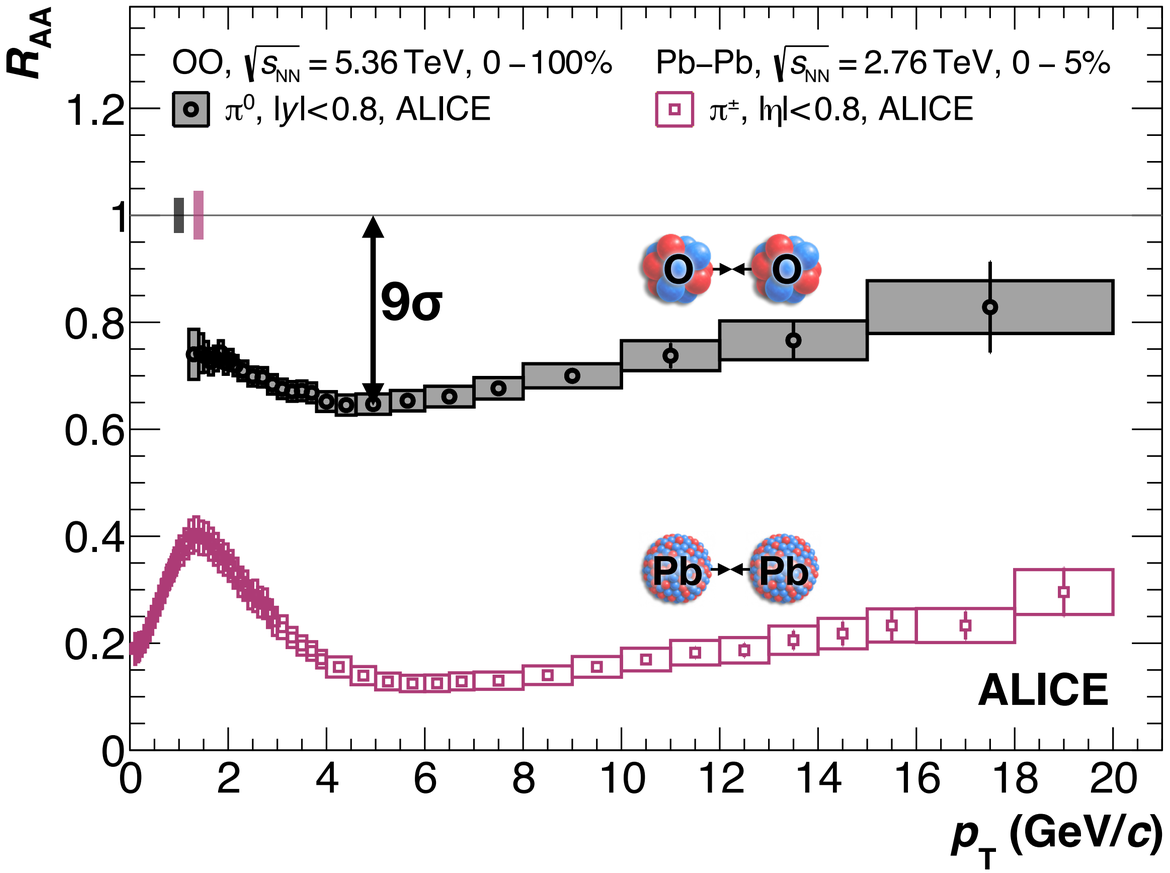
- R_{OO} significantly suppressed over full p_T range
  → **9σ** deviation from unity



Nuclear Modification of π^0 Production: R_{OO}

$$R_{AA} = \frac{1}{A^2}\frac{\sigma_{AA}}{\sigma_{pp}}$$

- R_{OO} significantly suppressed over full p_T range
  → **9σ** deviation from unity
- R_{OO} shape similar to R_{PbPb}
  → **Flow** at low p_T, rise towards unity at high p_T

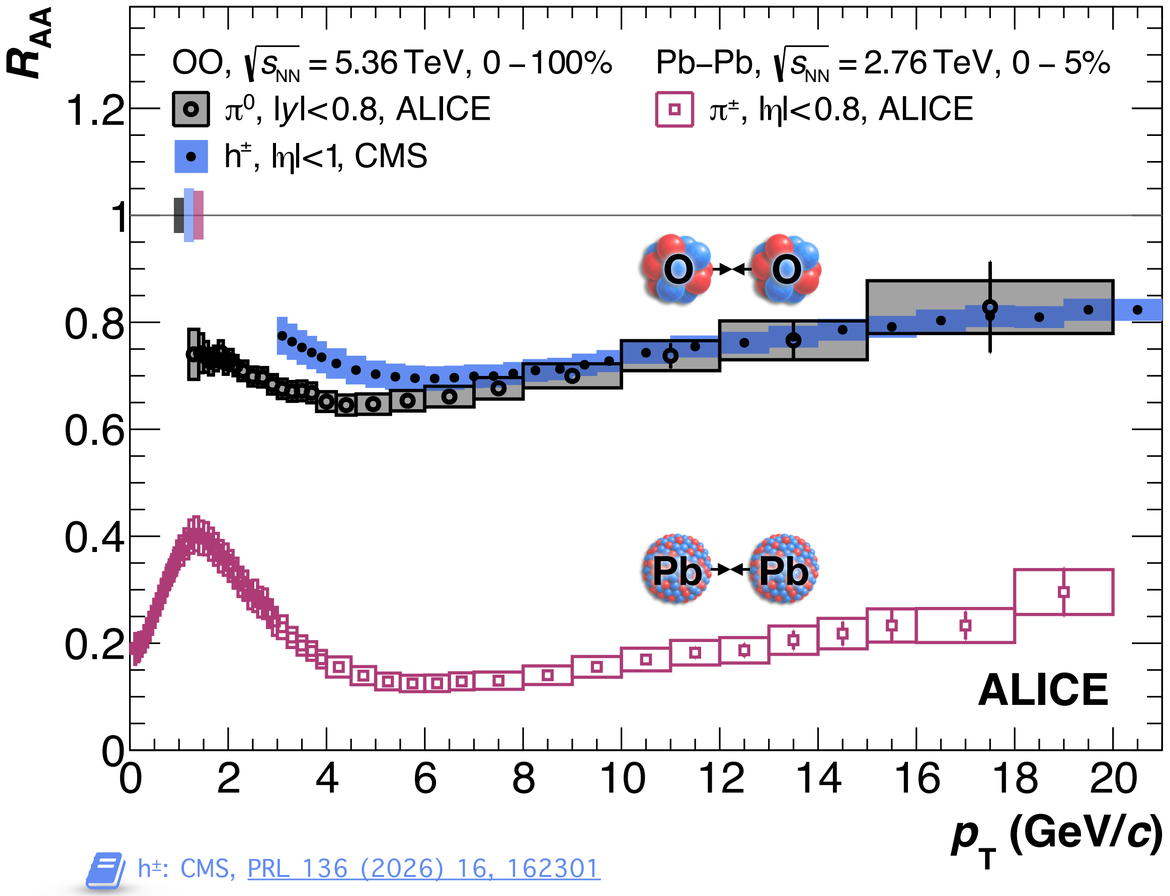


$\pi^{\pm}$: ALICE, PLB 736 (2014) 196-207

Nuclear Modification of π^0 Production: R_{OO}

$$R_{AA} = \frac{1}{A^2}\frac{\sigma_{AA}}{\sigma_{pp}}$$

- R_{OO} significantly suppressed over full p_T range
  → **9σ** deviation from unity
- R_{OO} shape similar to R_{PbPb}
  → **Flow** at low p_T, rise towards unity at high p_T
- Similar suppression observed by CMS



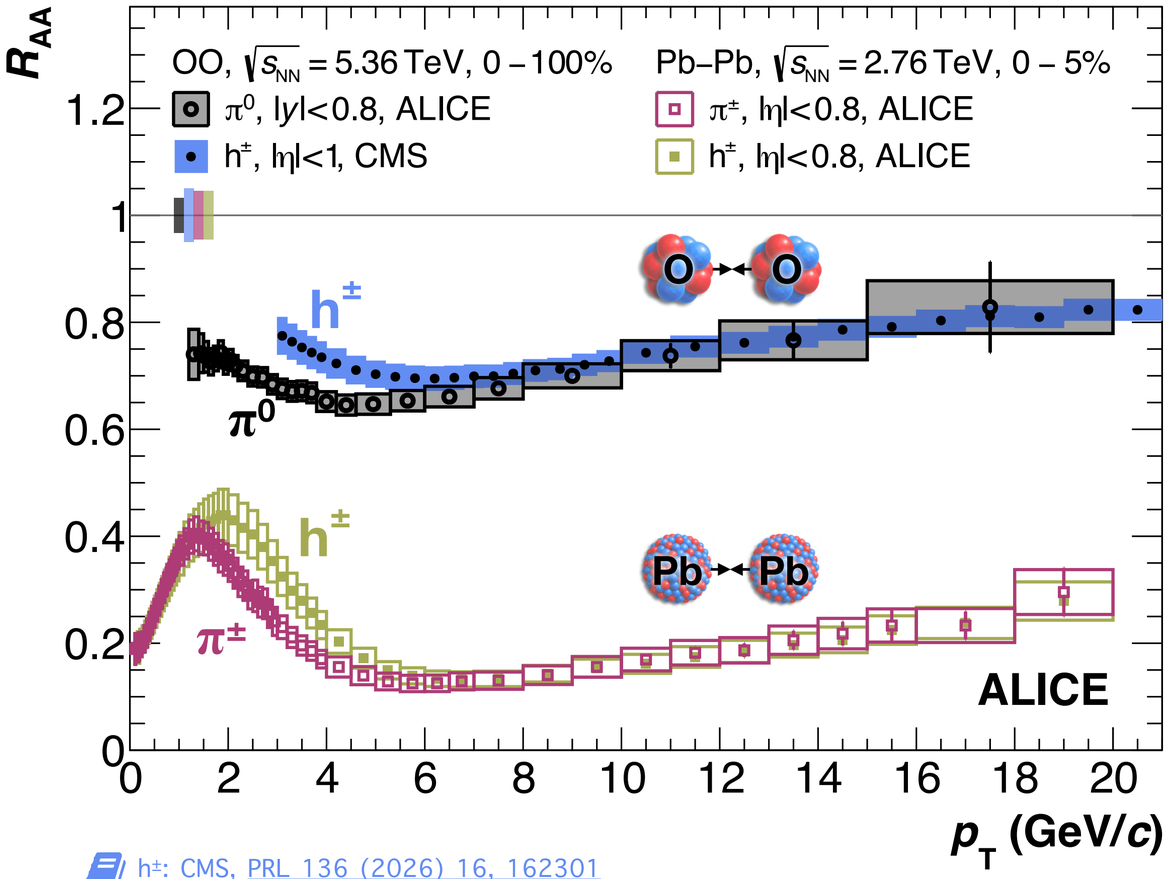
$h^{\pm}$: CMS, PRL 136 (2026) 16, 162301

$\pi^{\pm}$: ALICE, PLB 736 (2014) 196-207

Nuclear Modification of π^0 Production: R_{OO}

$$R_{AA} = \frac{1}{A^2}\frac{\sigma_{AA}}{\sigma_{pp}}$$

- R_{OO} significantly suppressed over full p_T range
  → **9σ** deviation from unity
- R_{OO} shape similar to R_{PbPb}
  → **Flow** at low p_T, rise towards unity at high p_T
- Similar suppression observed by CMS
- Difference at low p_T from different masses ($h^{\pm}/\pi^0$)



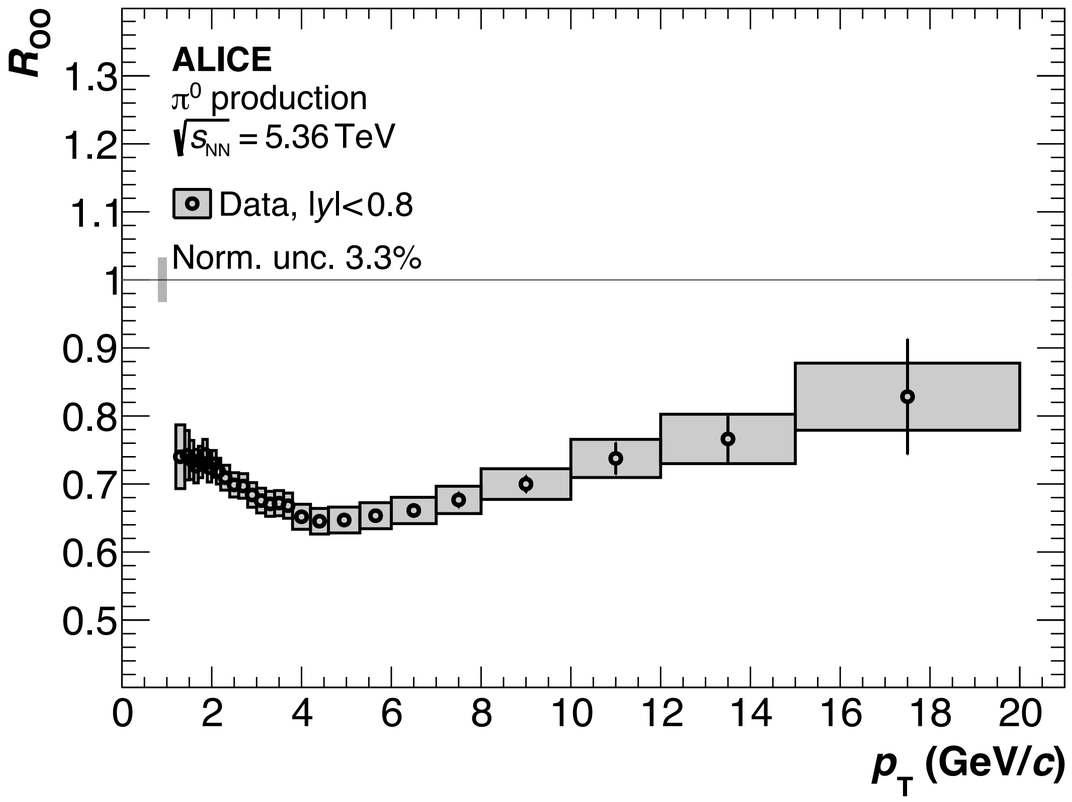
$h^{\pm}$: CMS, PRL 136 (2026) 16, 162301

$\pi^{\pm}$: ALICE, PLB 736 (2014) 196-207

$h^{\pm}$: ALICE, PLB 720 (2013) 52–62

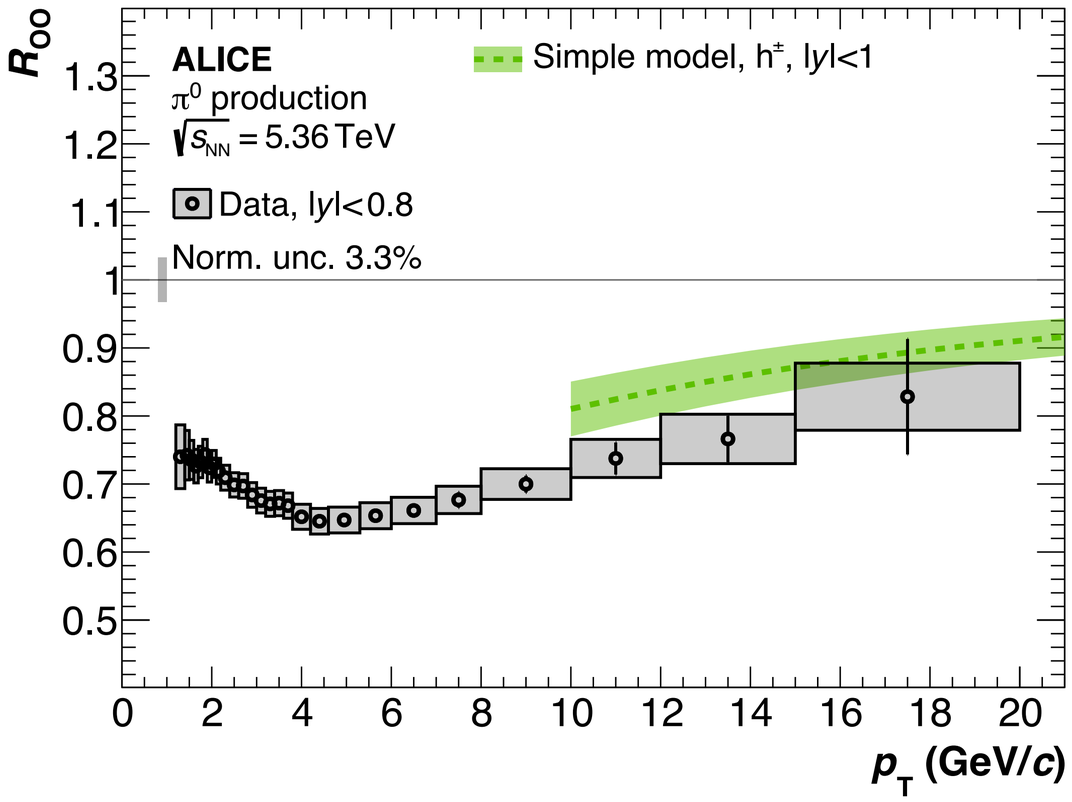
R_{OO} - Energy Loss Models

$$R_{AA} = \frac{1}{A^2}\frac{\sigma_{AA}}{\sigma_{pp}}$$



R_{OO} - Energy Loss Models

$$R_{AA} = \frac{1}{A^2}\frac{\sigma_{AA}}{\sigma_{pp}}$$

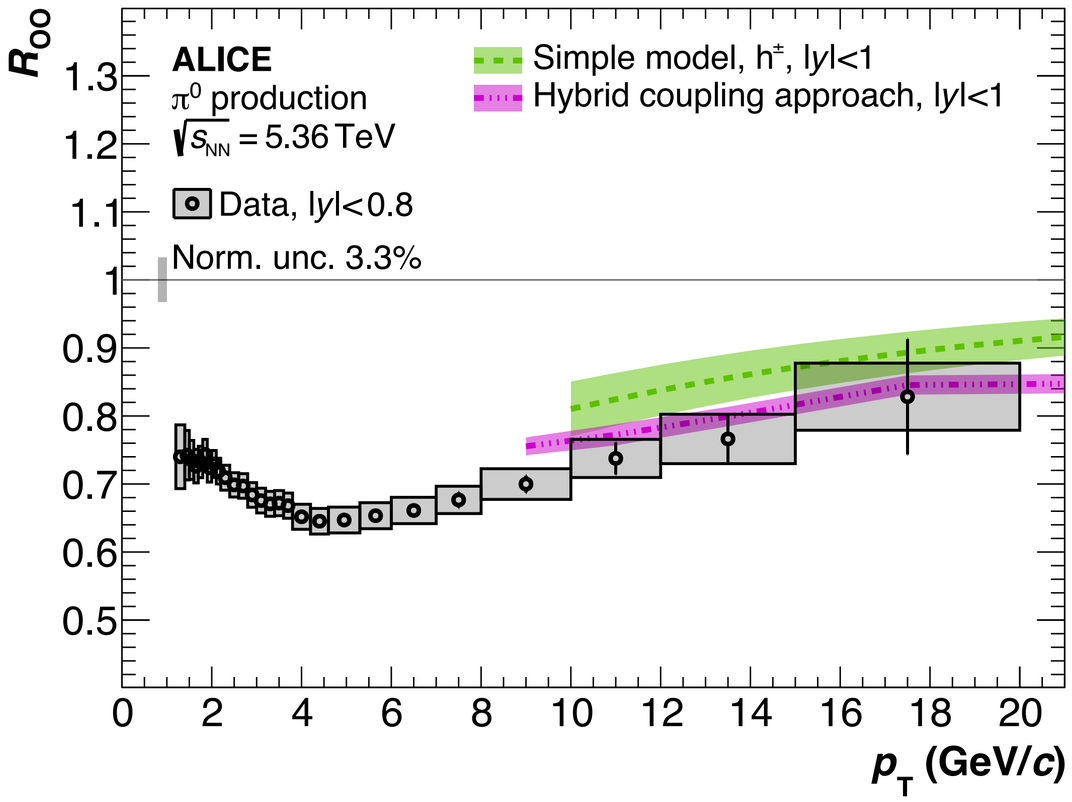


Simple model W. van der Schee et al., ariXiv:2509.04299

- BDMPS-Z energy loss with one free parameter $\hat{q}$
- CNM baseline: EPPS16

R_{OO} - Energy Loss Models

$$R_{AA} = \frac{1}{A^2}\frac{\sigma_{AA}}{\sigma_{pp}}$$



Simple model W. van der Schee et al., ariXiv:2509.04299

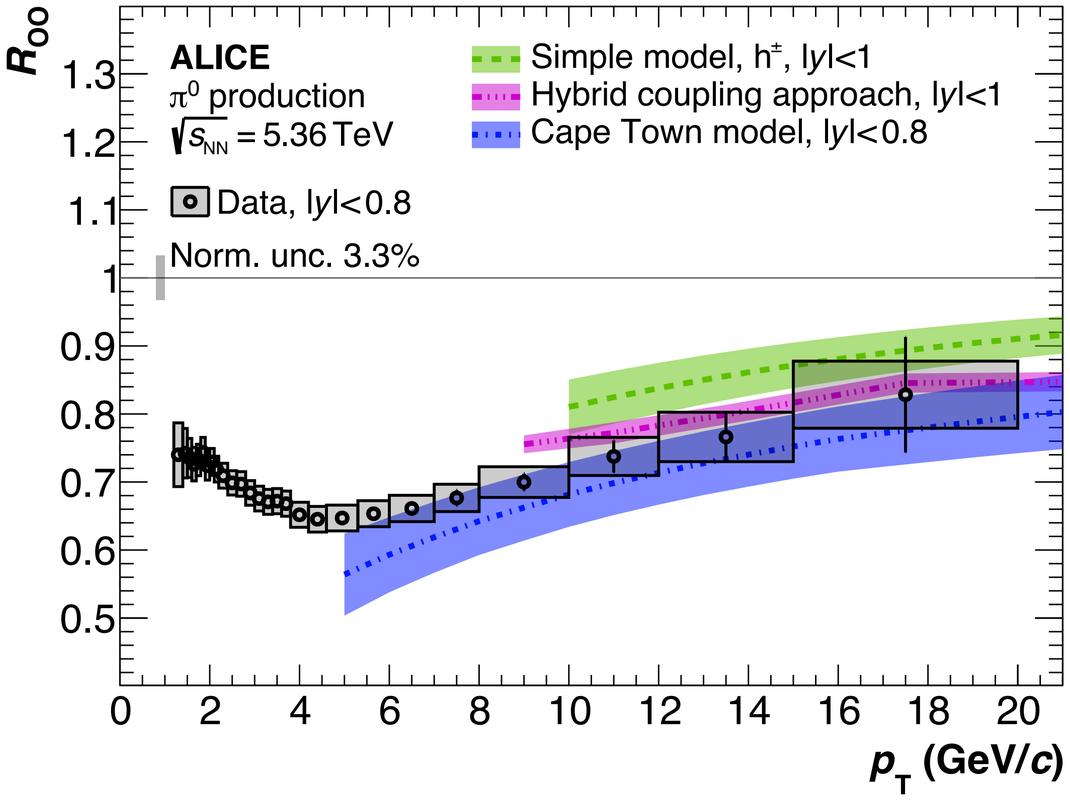
- BDMPS-Z energy loss with one free parameter $\hat{q}$
- CNM baseline: EPPS16

Hybrid coupling model A. Kudinoor et al., arXiv:2603.23596

- Hybrid model interfaced with event-by-event fluctuations
- CNM baseline: EPPS21

R_{OO} - Energy Loss Models

$$R_{AA} = \frac{1}{A^2}\frac{\sigma_{AA}}{\sigma_{pp}}$$



Simple model W. van der Schee et al., ariXiv:2509.04299

- BDMPS-Z energy loss with one free parameter $\hat{q}$
- CNM baseline: EPPS16

Hybrid coupling model A. Kudinoor et al., arXiv:2603.23596

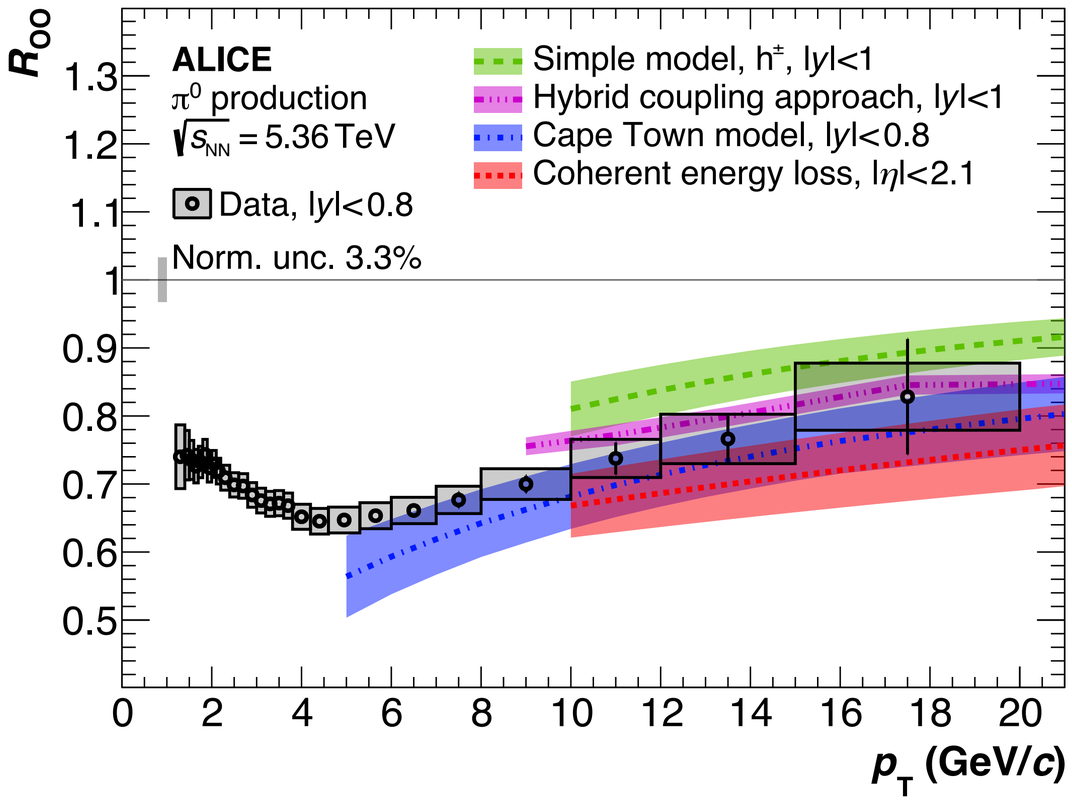
- Hybrid model interfaced with event-by-event fluctuations
- CNM baseline: EPPS21

Cape Town model C. Faraday and W. Horowitz, JHEP 11 (2025) 19

- Coll. + rad. energy loss, constrained by central heavy ion data
- No CNM effects included

R_{OO} - Energy Loss Models

$$R_{AA} = \frac{1}{A^2}\frac{\sigma_{AA}}{\sigma_{pp}}$$



Simple model W. van der Schee et al., ariXiv:2509.04299

- BDMPS-Z energy loss with one free parameter $\hat{q}$
- CNM baseline: EPPS16

Hybrid coupling model A. Kudinoor et al., arXiv:2603.23596

- Hybrid model interfaced with event-by-event fluctuations
- CNM baseline: EPPS21

Cape Town model C. Faraday and W. Horowitz, JHEP 11 (2025) 19

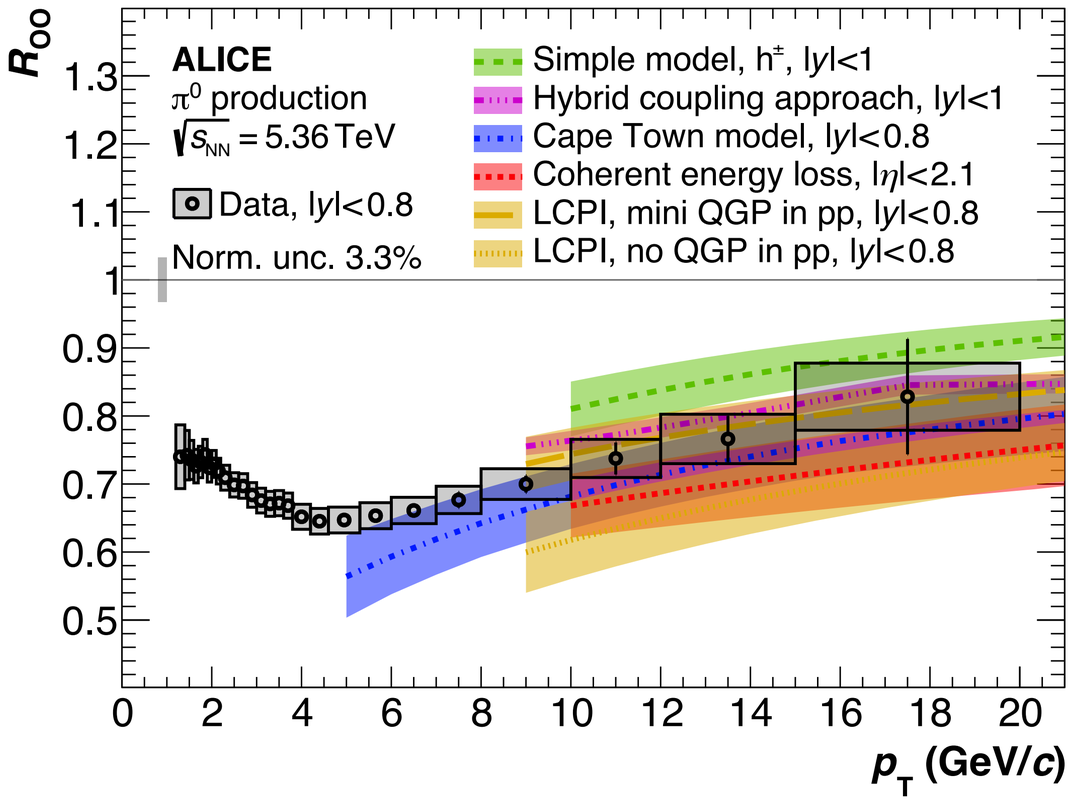
- Coll. + rad. energy loss, constrained by central heavy ion data
- No CNM effects included

Coherent energy loss D. Pablos and A. Takacs, PRC 113 (2026) 044913

- Semi-analytic jet quenching with CEL in medium
- CNM baseline: EPPS21

R_{OO} - Energy Loss Models

$$R_{AA} = \frac{1}{A^2}\frac{\sigma_{AA}}{\sigma_{pp}}$$



Simple model — W. van der Schee et al., ariXiv:2509.04299

- BDMPS-Z energy loss with one free parameter $\hat{q}$
- CNM baseline: EPPS16

Hybrid coupling model — A. Kudinoor et al., arXiv:2603.23596

- Hybrid model interfaced with event-by-event fluctuations
- CNM baseline: EPPS21

Cape Town model — C. Faraday and W. Horowitz, JHEP 11 (2025) 19

- Coll. + rad. energy loss, constrained by central heavy ion data
- No CNM effects included

Coherent energy loss — D. Pablos and A. Takacs, PRC 113 (2026) 044913

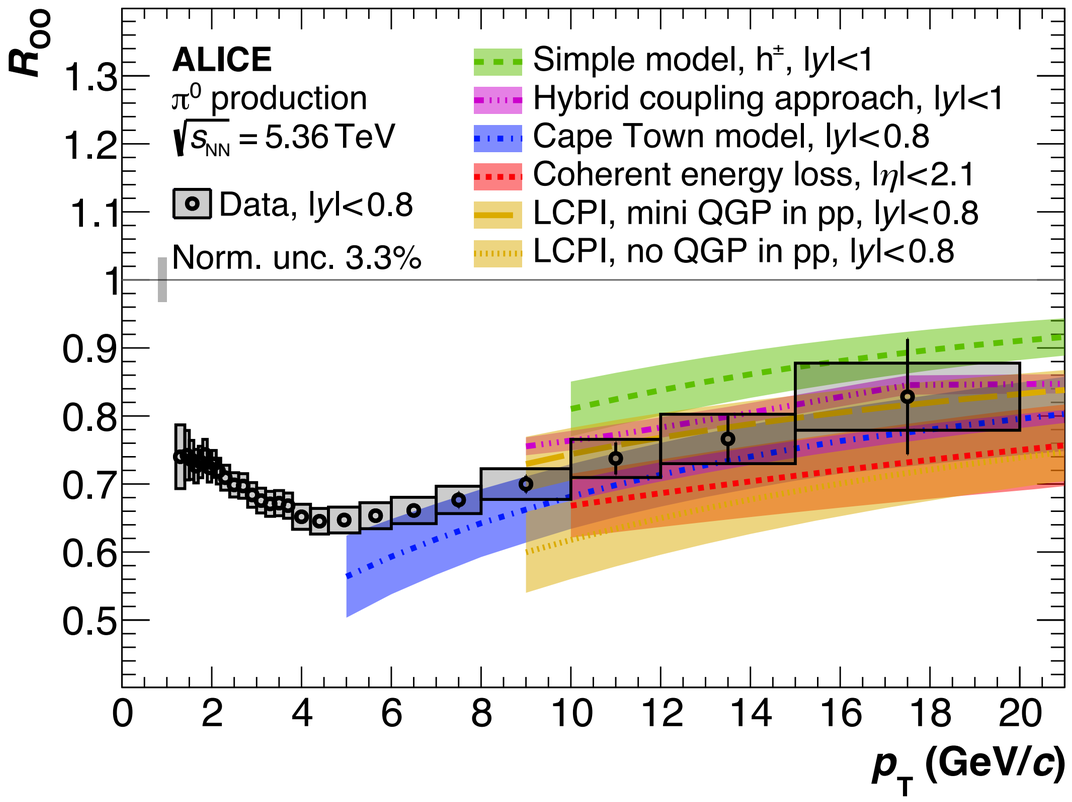
- Semi-analytic jet quenching with CEL in medium
- CNM baseline: EPPS21

Light-Cone Path Integral — B.G. Zakharov, JHEP 09 (2021) 087

- 2 scenarios: With and without a mini QGP in pp
- CNM baseline: EPS09

R_{OO} - Energy Loss Models

$$R_{AA} = \frac{1}{A^2}\frac{\sigma_{AA}}{\sigma_{pp}}$$



➡ Influence of different CNM inputs?

Simple model — W. van der Schee et al., ariXiv:2509.04299

- BDMPS-Z energy loss with one free parameter $\hat{q}$
- CNM baseline: EPPS16

Hybrid coupling model — A. Kudinoor et al., arXiv:2603.23596

- Hybrid model interfaced with event-by-event fluctuations
- CNM baseline: EPPS21

Cape Town model — C. Faraday and W. Horowitz, JHEP 11 (2025) 19

- Coll. + rad. energy loss, constrained by central heavy ion data
- No CNM effects included

Coherent energy loss — D. Pablos and A. Takacs, PRC 113 (2026) 044913

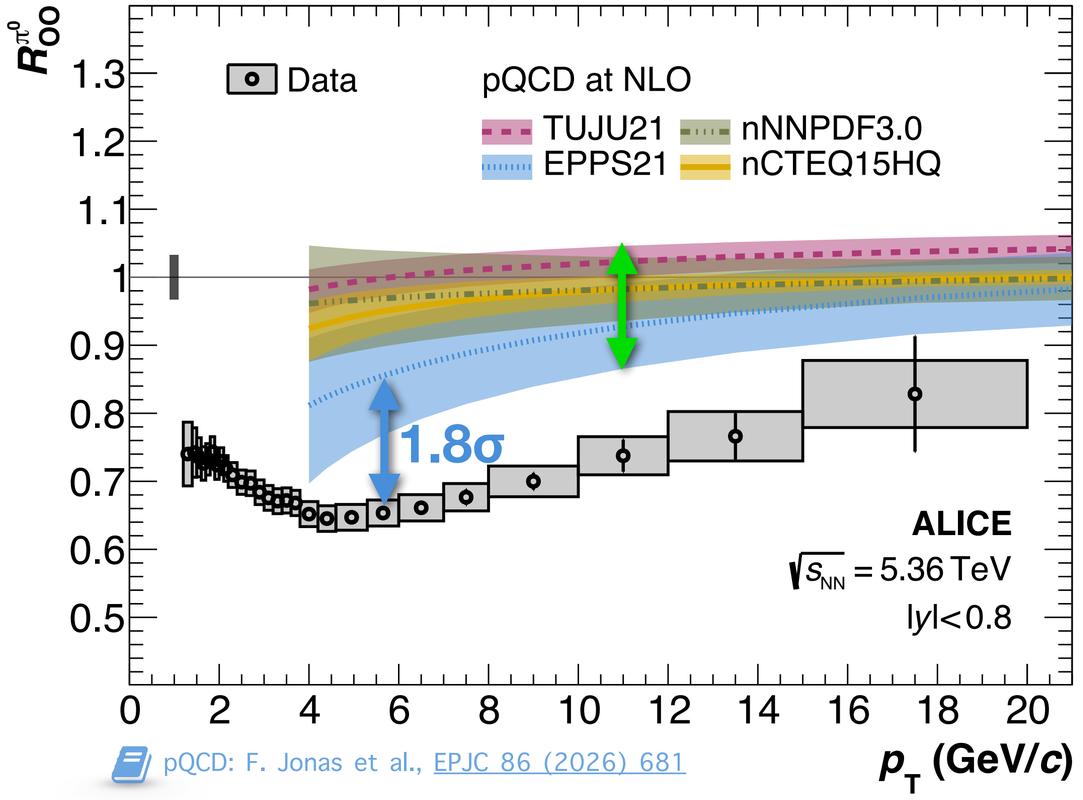
- Semi-analytic jet quenching with CEL in medium
- CNM baseline: EPPS21

Light-Cone Path Integral — B.G. Zakharov, JHEP 09 (2021) 087

- 2 scenarios: With and without a mini QGP in pp
- CNM baseline: EPS09

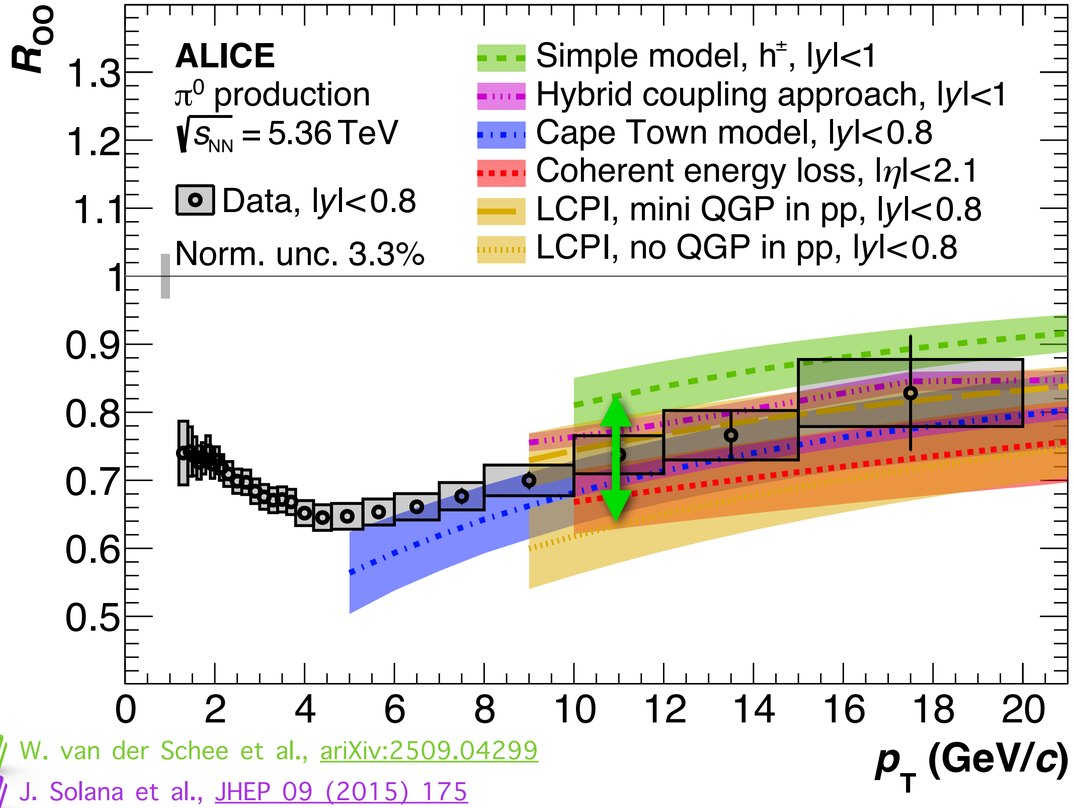
Impact of CNM Effects on R_{OO}

- Large uncertainties and spread between nPDFs → **~20%** uncertainty on CNM suppression of R_{OO}
- Significance of suppression w.r.t. nPDFs only **1.8σ** → R_{OO} suppression explainable through CNM?

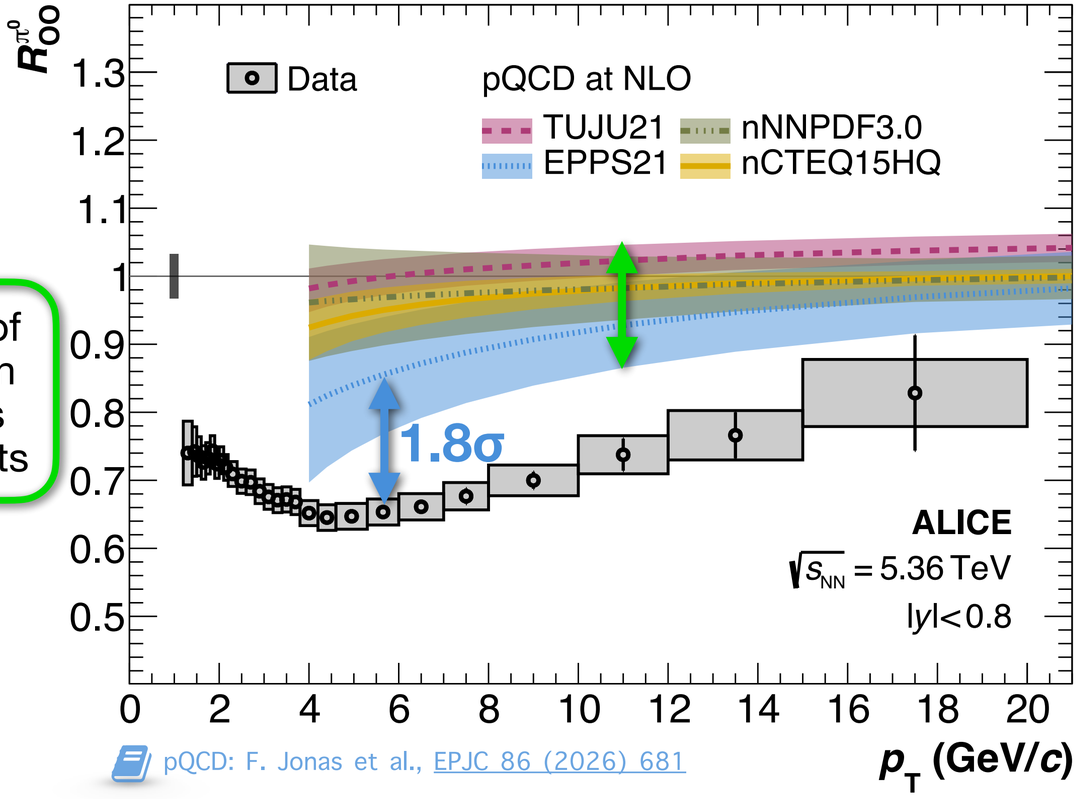


Impact of CNM Effects on R_{OO}

- Large uncertainties and spread between nPDFs → **~20%** uncertainty on CNM suppression of R_{OO}
- Significance of suppression w.r.t. nPDFs only **1.8σ** → R_{OO} suppression explainable through CNM?



Same spread of ~20% between e-loss models and nPDF inputs

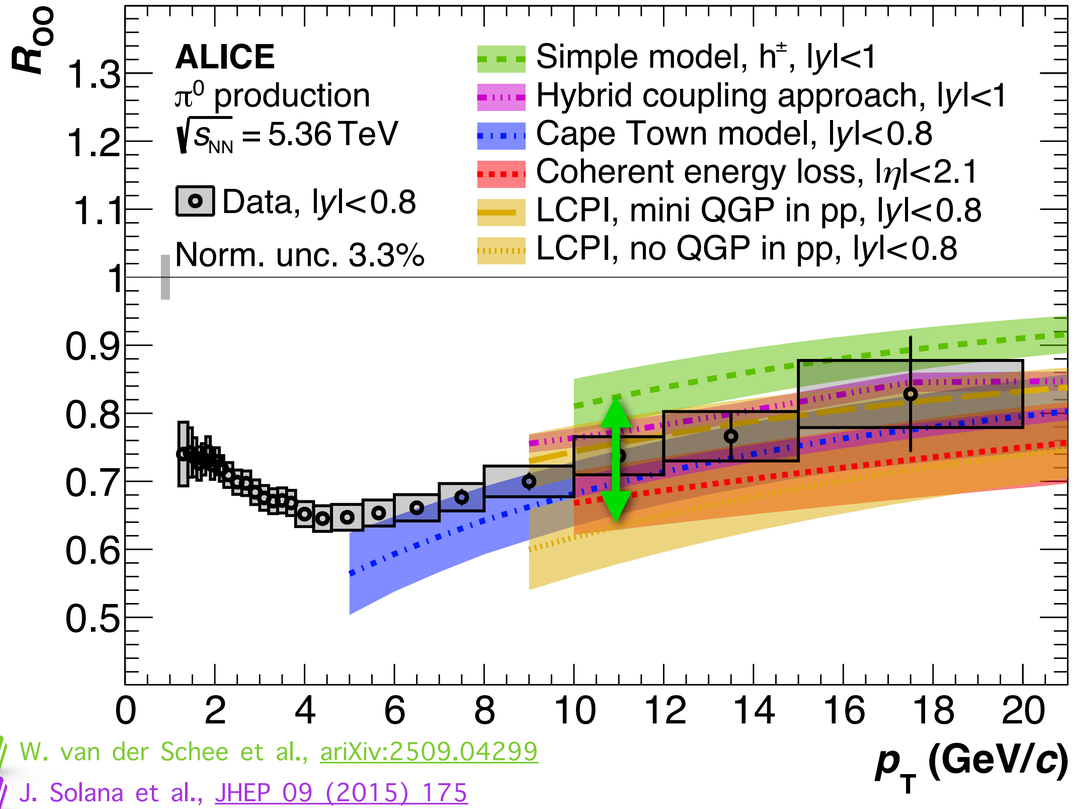


W. van der Schee et al., ariXiv:2509.04299
J. Solana et al., JHEP 09 (2015) 175
C. Faraday and W. Horowitz, JHEP 11 (2025) 19
D. Pablos and A. Takacs, PRC 113 (2026) 044913
B.G. Zakharov, JHEP 09 (2021) 087

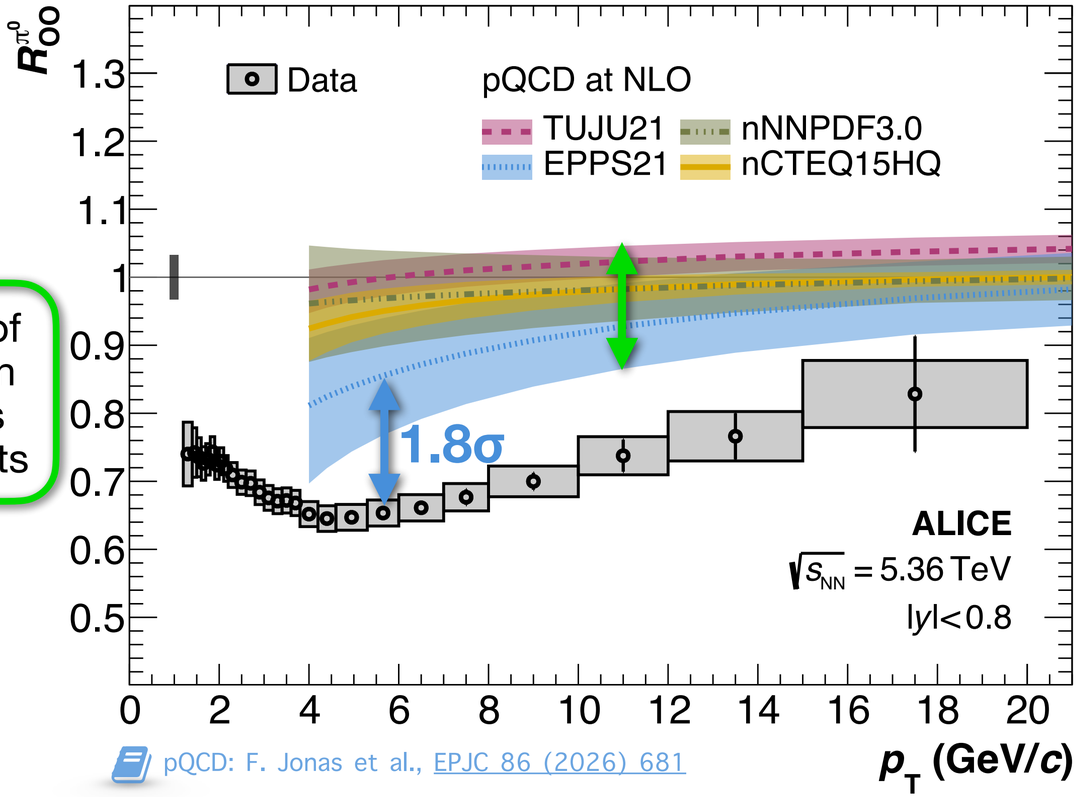
pQCD: F. Jonas et al., EPJC 86 (2026) 681

Impact of CNM Effects on R_{OO}

- Large uncertainties and spread between nPDFs → **~20%** uncertainty on CNM suppression of R_{OO}
- Significance of suppression w.r.t. nPDFs only **1.8σ** → R_{OO} suppression explainable through CNM?



Same spread of ~20% between e-loss models and nPDF inputs



W. van der Schee et al., ariXiv:2509.04299
J. Solana et al., JHEP 09 (2015) 175
C. Faraday and W. Horowitz, JHEP 11 (2025) 19
D. Pablos and A. Takacs, PRC 113 (2026) 044913
B.G. Zakharov, JHEP 09 (2021) 087

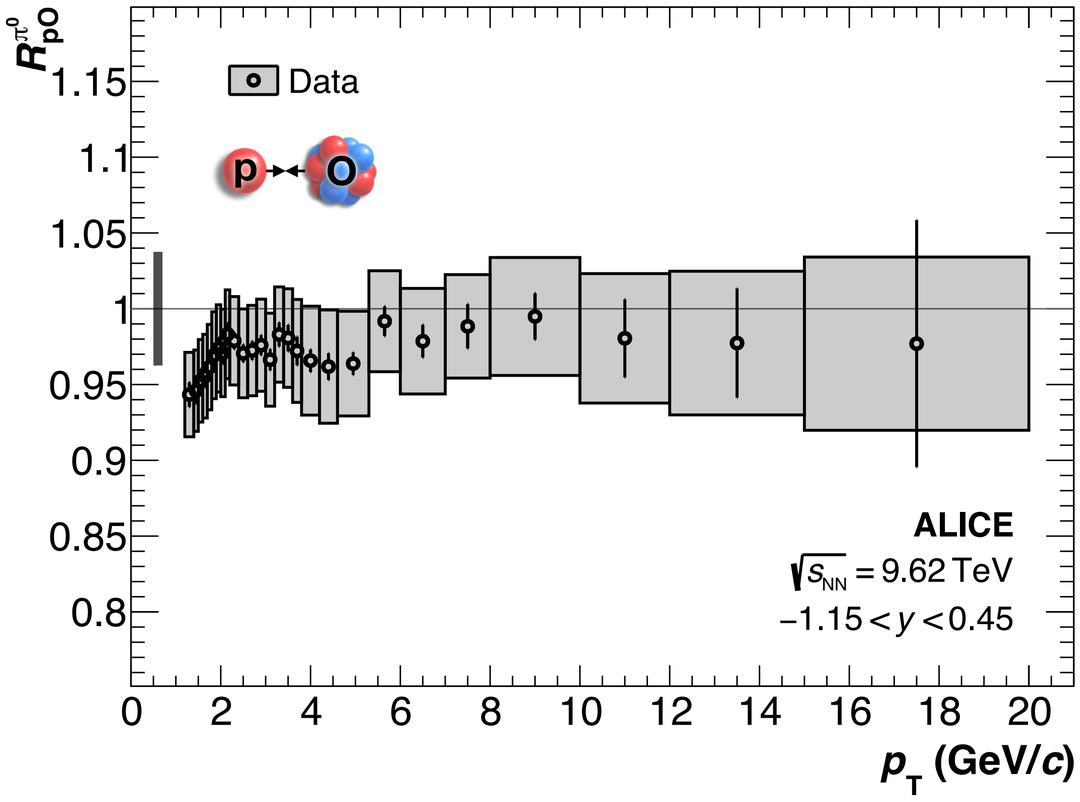
pQCD: F. Jonas et al., EPJC 86 (2026) 681

➡ nPDF uncertainties don't allow for assessment of energy-loss description!

First CNM Constraints in Oxygen: R_{pO}

- R_{pO} consistent with unity over full p_{T} range
- Hint of suppression at low $p_{\mathrm{T}} < 2$ GeV/c

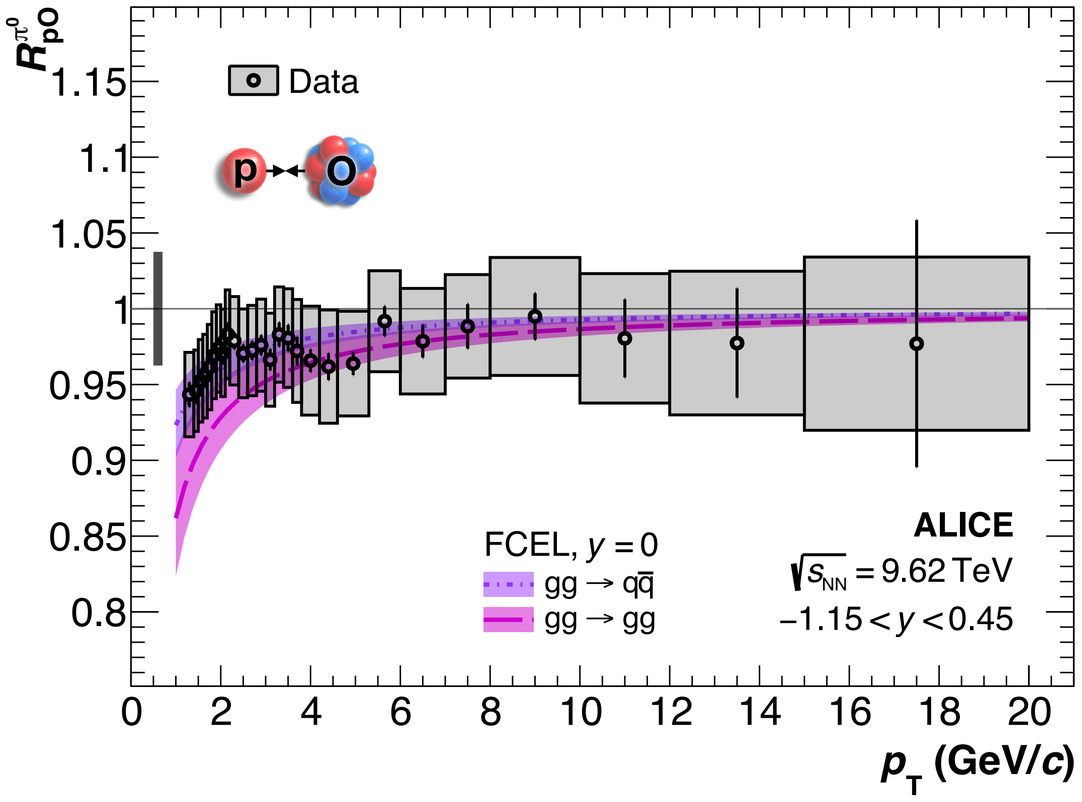
$$R_{\mathrm{pO}} = \frac{1}{A}\frac{\sigma_{\mathrm{pO}}}{\sigma_{\mathrm{pp}}}$$



First CNM Constraints in Oxygen: R_{pO}

- R_{pO} consistent with unity over full p_{T} range
- Hint of suppression at low $p_{\mathrm{T}} < 2$ GeV/c
- Fully Coherent Energy Loss (FCEL) describes data including shape at low p_{T}

$$R_{\mathrm{pO}} = \frac{1}{A}\frac{\sigma_{\mathrm{pO}}}{\sigma_{\mathrm{pp}}}$$

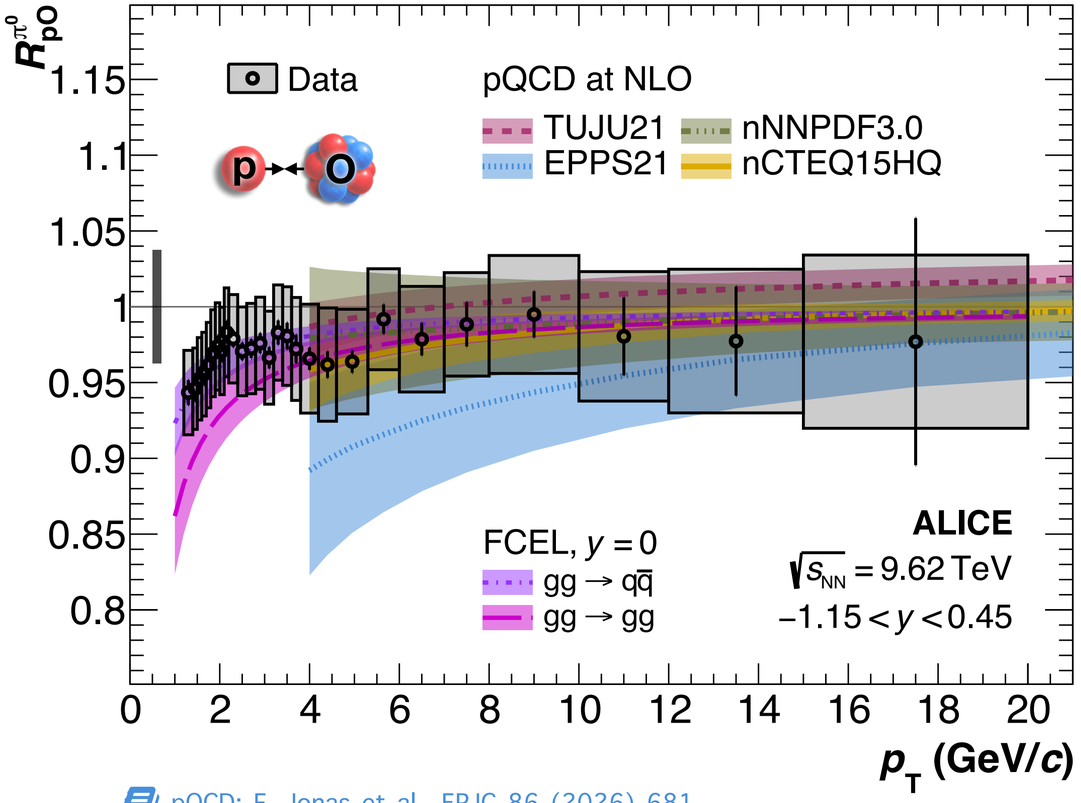


FCEL: F. Arleo and S. Peigne, PRL 125, 032301 (2020)

First CNM Constraints in Oxygen: R_{pO}

- R_{pO} consistent with unity over full p_T range
- Hint of suppression at low $p_T < 2$ GeV/c
- Fully Coherent Energy Loss (FCEL) describes data including shape at low p_T
- nPDF predictions compatible with data within large model uncertainties

$$R_{pO} = \frac{1}{A}\frac{\sigma_{pO}}{\sigma_{pp}}$$

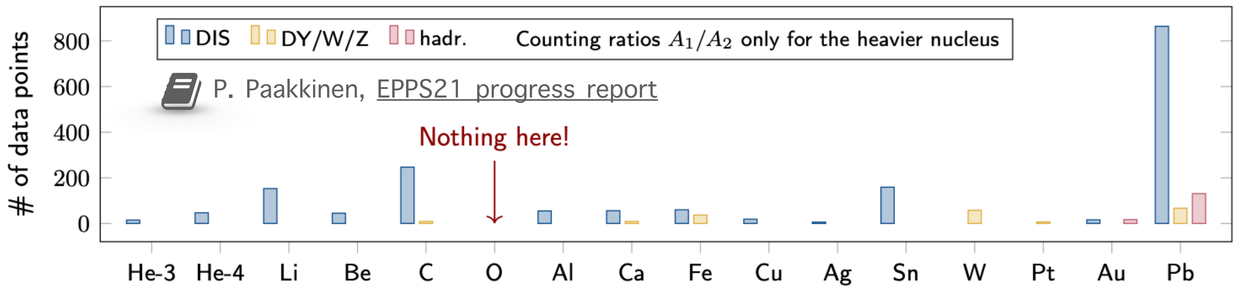


pQCD: F. Jonas et al., EPJC 86 (2026) 681

FCEL: F. Arleo and S. Peigne, PRL 125, 032301 (2020)

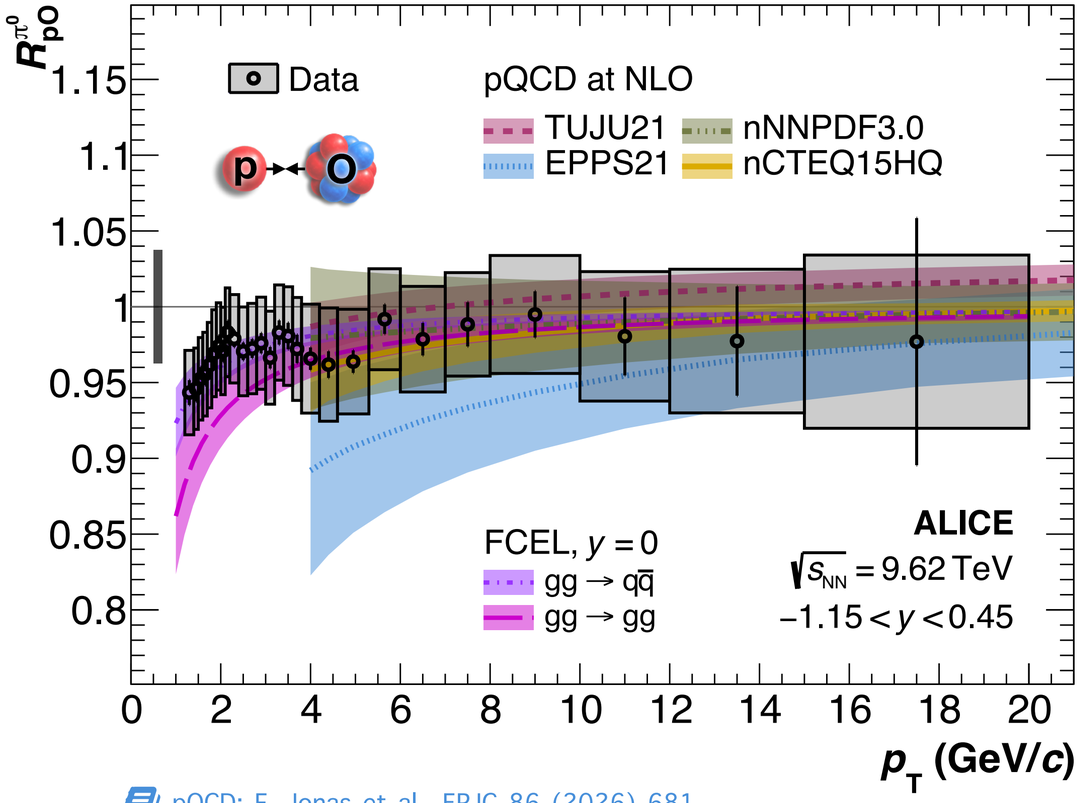
First CNM Constraints in Oxygen: R_{pO}

- R_{pO} consistent with unity over full p_T range
- Hint of suppression at low $p_T < 2$ GeV/c
- Fully Coherent Energy Loss (FCEL) describes data including shape at low p_T
- nPDF predictions compatible with data within large model uncertainties



→ Complete lack of experimental input — so far

$$R_{pO} = \frac{1}{A}\frac{\sigma_{pO}}{\sigma_{pp}}$$



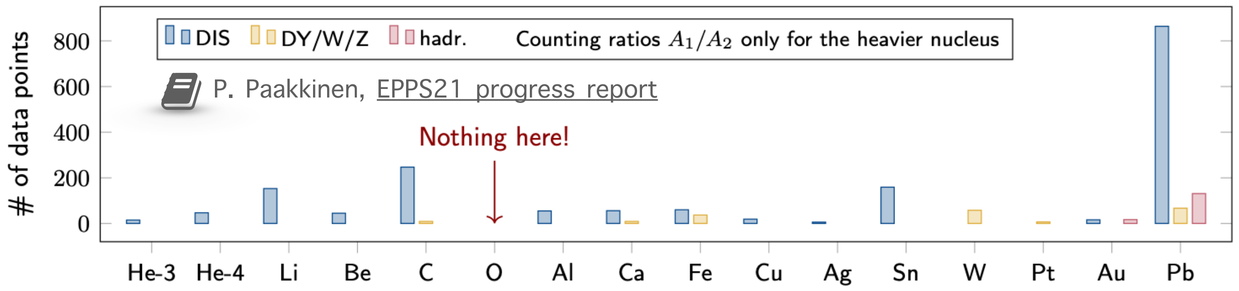
pQCD: F. Jonas et al., EPJC 86 (2026) 681

FCEL: F. Arleo and S. Peigne, PRL 125, 032301 (2020)

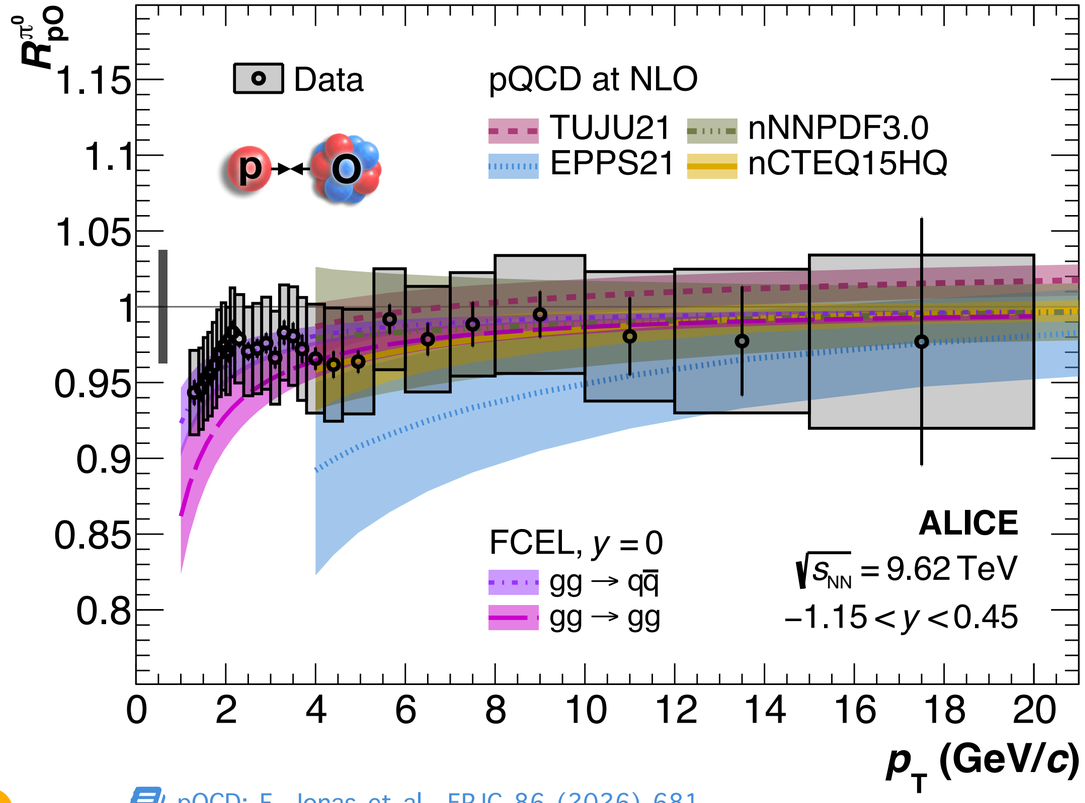
First CNM Constraints in Oxygen: R_{pO}

- R_{pO} consistent with unity over full p_T range
- Hint of suppression at low $p_T < 2$ GeV/c
- Fully Coherent Energy Loss (FCEL) describes data including shape at low p_T
- nPDF predictions compatible with data within large model uncertainties

$$R_{pO} = \frac{1}{A}\frac{\sigma_{pO}}{\sigma_{pp}}$$



→ Complete lack of experimental input — so far

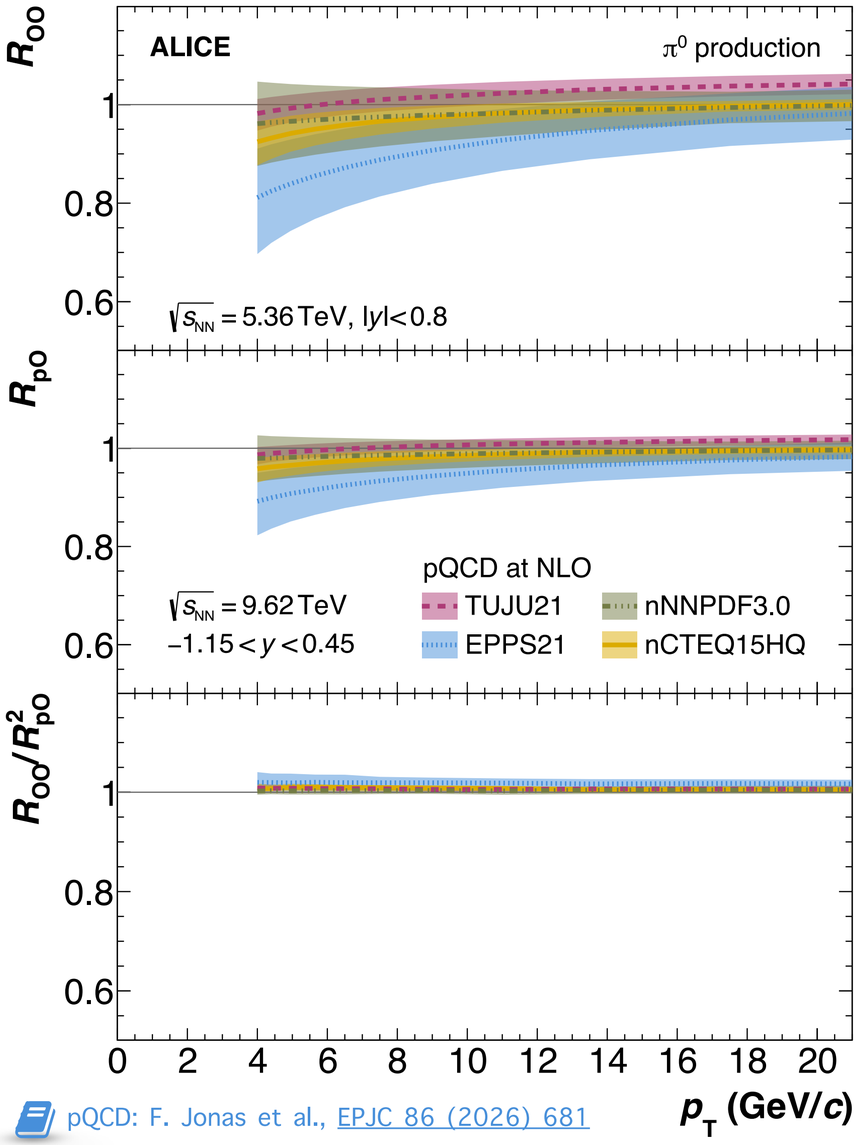


pQCD: F. Jonas et al., EPJC 86 (2026) 681

FCEL: F. Arleo and S. Peigne, PRL 125, 032301 (2020)

➡ Providing first constraints on CNM effects in oxygen

Cancelling CNM Effects: R_{OO}/R_{pO}^2



pQCD: F. Jonas et al., EPJC 86 (2026) 681

The idea

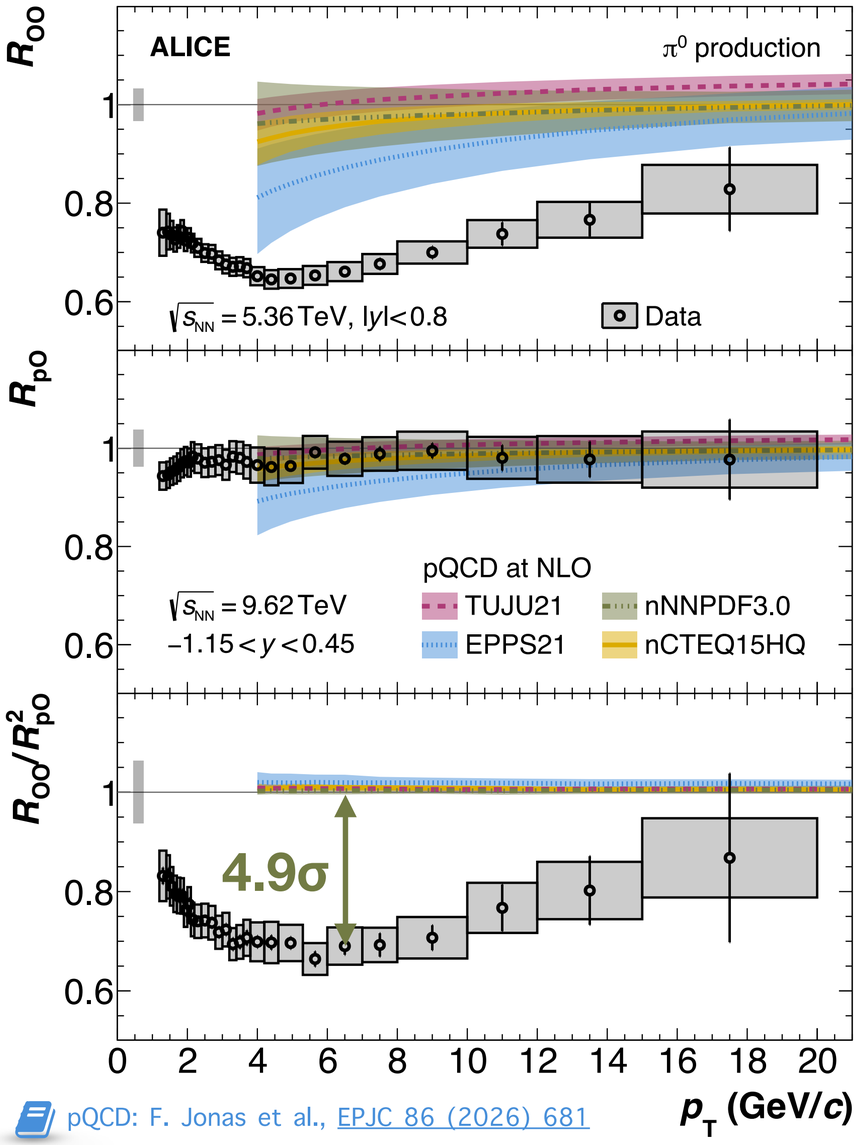
- R_{OO} contains CNM effects of 2 oxygen nuclei
- R_{pO} contains CNM effects of 1 oxygen nucleus

→ R_{OO}/R_{pO}^2 does not contain any CNM effects

nPDF predictions for R_{OO}/R_{pO}^2

- Slightly above unity (different $\sqrt{s_{NN}}$ and y)
- Excellent cancellation of CNM effects and uncertainties
  → ~1% model uncertainties (instead of ~10% on R_{OO})

Cancelling CNM Effects: R_{OO}/R_{pO}^2



pQCD: F. Jonas et al., EPJC 86 (2026) 681

The idea

- R_{OO} contains CNM effects of 2 oxygen nuclei
- R_{pO} contains CNM effects of 1 oxygen nucleus

→ R_{OO}/R_{pO}^2 does not contain any CNM effects

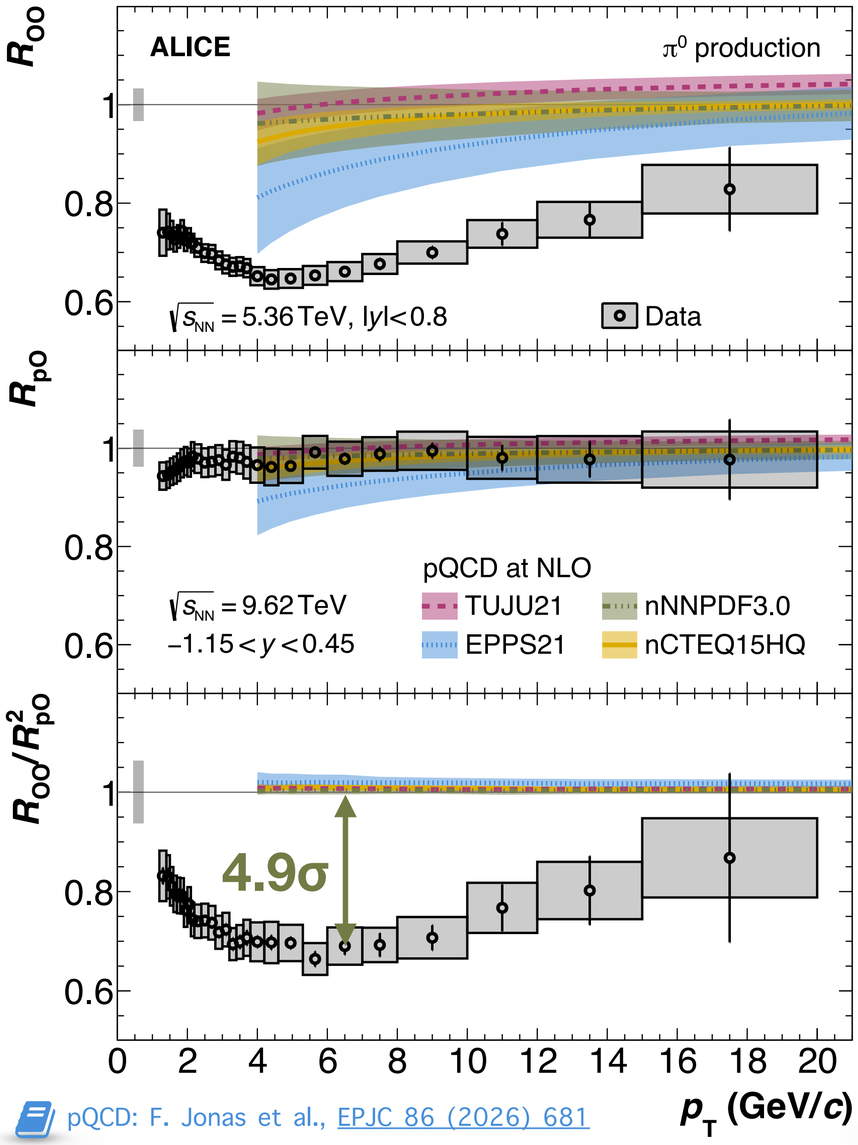
nPDF predictions for R_{OO}/R_{pO}^2

- Slightly above unity (different $\sqrt{s_{NN}}$ and y)
- Excellent cancellation of CNM effects and uncertainties
  → ~1% model uncertainties (instead of ~10% on R_{OO})

Data

- Measured R_{OO}/R_{pO}^2 looks similar to R_{OO}
- Deviation from nPDF baselines: > **4.9σ**

Cancelling CNM Effects: R_{OO}/R_{pO}^2



pQCD: F. Jonas et al., EPJC 86 (2026) 681

The idea

- R_{OO} contains CNM effects of 2 oxygen nuclei
- R_{pO} contains CNM effects of 1 oxygen nucleus

→ R_{OO}/R_{pO}^2 does not contain any CNM effects

nPDF predictions for R_{OO}/R_{pO}^2

- Slightly above unity (different $\sqrt{s_{NN}}$ and y)
- Excellent cancellation of CNM effects and uncertainties
  → ~1% model uncertainties (instead of ~10% on R_{OO})

Data

- Measured R_{OO}/R_{pO}^2 looks similar to R_{OO}
- Deviation from nPDF baselines: > **4.9σ**

➡ 4.9σ evidence for energy loss in oxygen-oxygen collisions

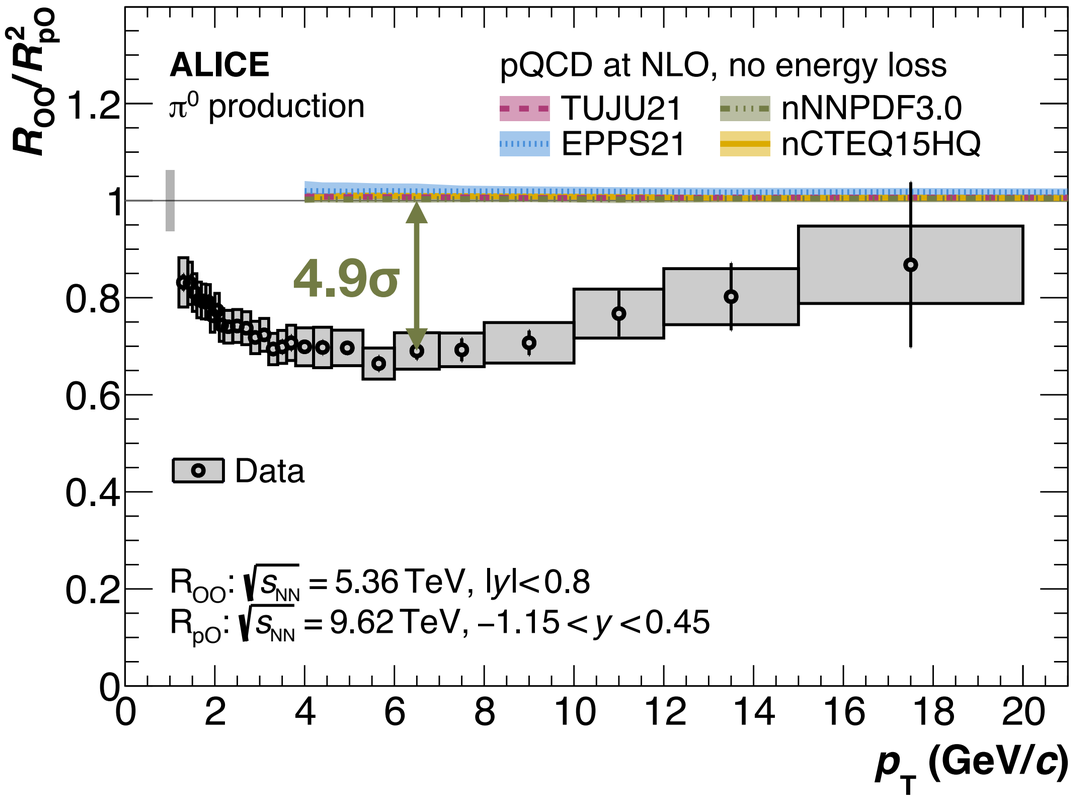
Probing Parton Energy Loss using R_{OO}/R_{pO}^2

Data significantly below predictions without energy loss:

- **4.9σ** from nNNPDF3.0
- 5.0σ from TUJU21, EPPS21 and nCTEQ15HQ

→ **4.9σ evidence for parton energy loss in OO**

R_{OO}/R_{pO}^2 contains no CNM effects
→ **Direct probe of energy loss**



pQCD: F. Jonas et al., EPJC 86 (2026) 681

Probing Parton Energy Loss using R_{OO}/R_{pO}^2

Data significantly below predictions without energy loss:

- **4.9σ** from nNNPDF3.0
- 5.0σ from TUJU21, EPPS21 and nCTEQ15HQ

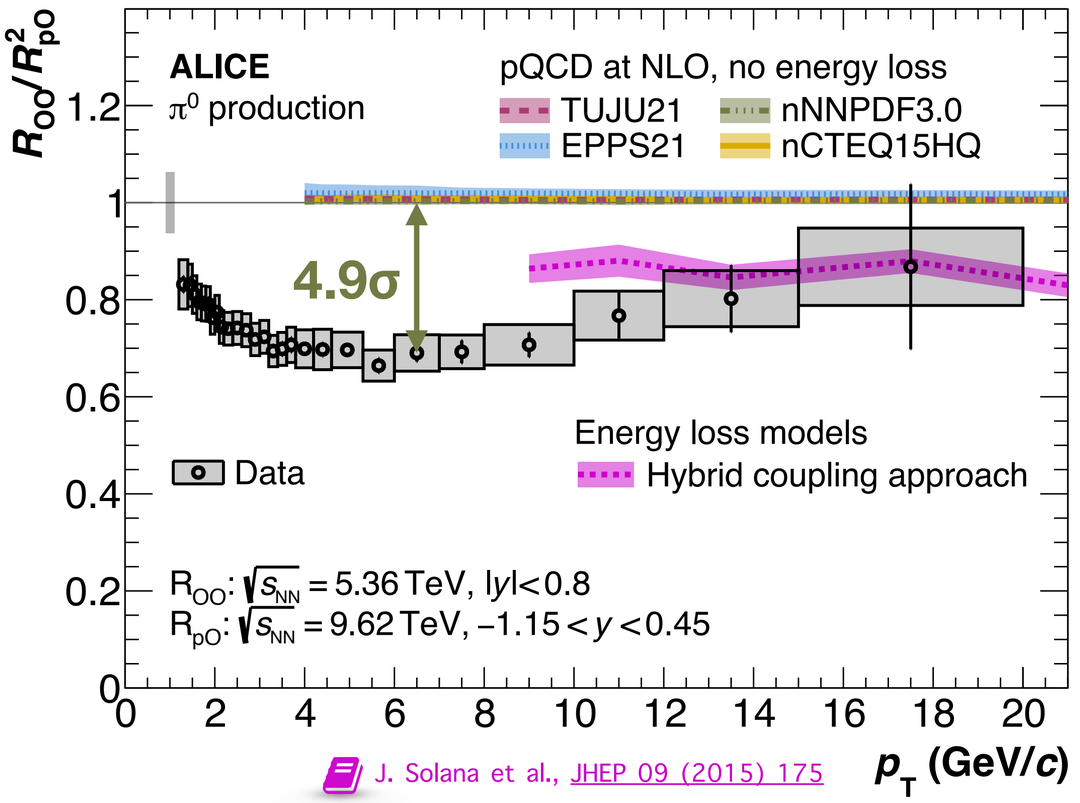
→ **4.9σ evidence for parton energy loss in OO**

R_{OO}/R_{pO}^2 contains no CNM effects
→ **Direct probe of energy loss**

Energy loss models:

Hybrid coupling model A. Kudinoor et al., arXiv:2603.23596

- Hybrid model interfaced with event-by-event fluctuations
- Including Molière scattering



J. Solana et al., JHEP 09 (2015) 175

pQCD: F. Jonas et al., EPJC 86 (2026) 681

Probing Parton Energy Loss using R_{OO}/R_{pO}^2

Data significantly below predictions without energy loss:

- **4.9σ** from nNNPDF3.0
- 5.0σ from TUJU21, EPPS21 and nCTEQ15HQ

→ **4.9σ evidence for parton energy loss in OO**

R_{OO}/R_{pO}^2 contains no CNM effects
→ **Direct probe of energy loss**

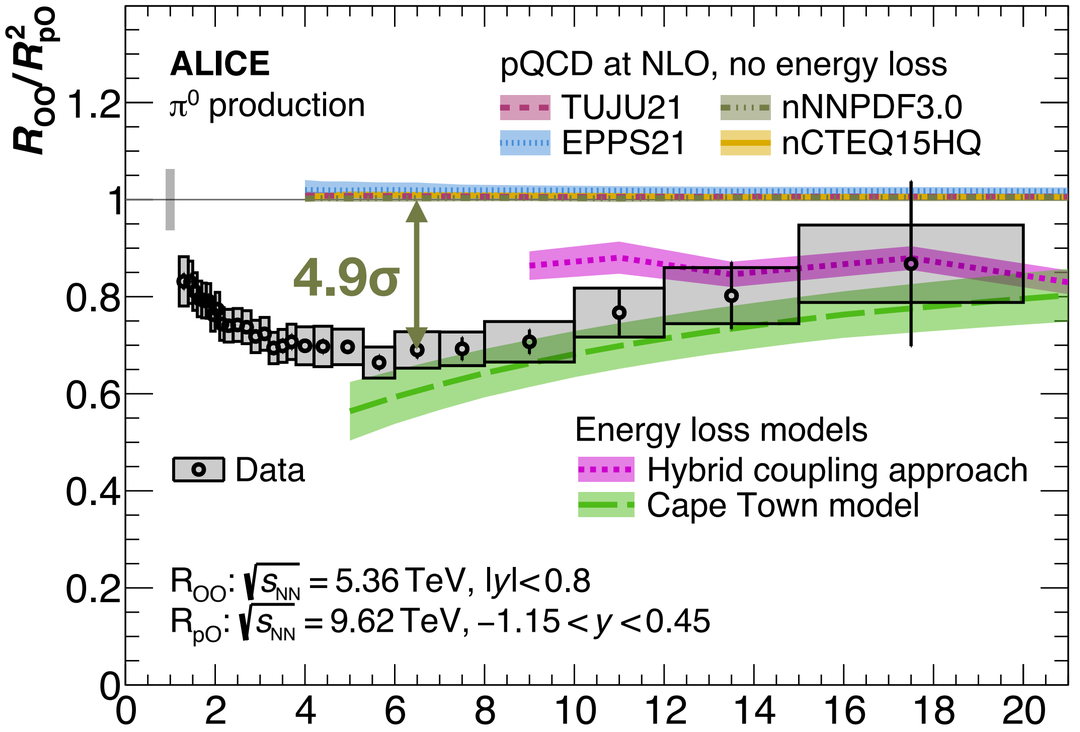
Energy loss models:

Hybrid coupling model A. Kudinoor et al., arXiv:2603.23596

- Hybrid model interfaced with event-by-event fluctuations
- Including Molière scattering

Cape Town model C. Faraday and W. Horowitz, JHEP 11 (2025) 19

- Collisional and radiative energy loss
- Including correction for small systems



J. Solana et al., JHEP 09 (2015) 175
C. Faraday and W. Horowitz, JHEP 11 (2025) 19
pQCD: F. Jonas et al., EPJC 86 (2026) 681

Probing Parton Energy Loss using R_{OO}/R_{pO}^2

Data significantly below predictions without energy loss:

- **4.9σ** from nNNPDF3.0
- 5.0σ from TUJU21, EPPS21 and nCTEQ15HQ

→ **4.9σ evidence for parton energy loss in OO**

R_{OO}/R_{pO}^2 contains no CNM effects
→ **Direct probe of energy loss**

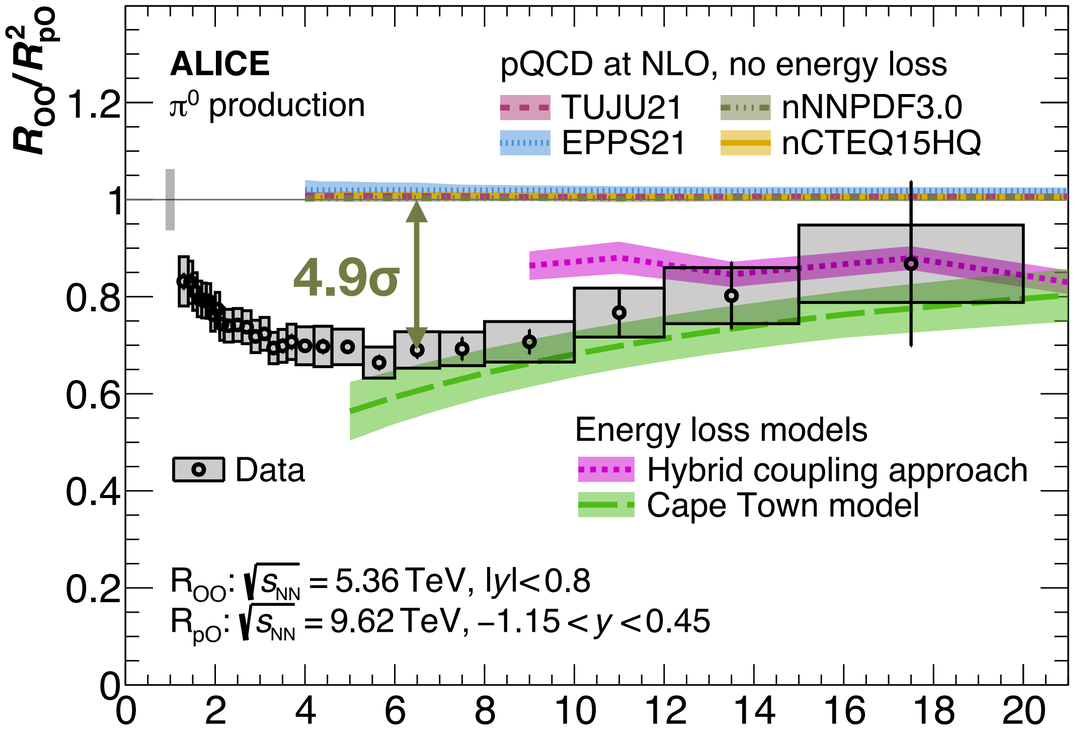
Energy loss models:

Hybrid coupling model A. Kudinoor et al., arXiv:2603.23596

- Hybrid model interfaced with event-by-event fluctuations
- Including Molière scattering

Cape Town model C. Faraday and W. Horowitz, JHEP 11 (2025) 19

- Collisional and radiative energy loss
- Including correction for small systems



J. Solana et al., JHEP 09 (2015) 175
C. Faraday and W. Horowitz, JHEP 11 (2025) 19
pQCD: F. Jonas et al., EPJC 86 (2026) 681

➡ Energy loss models capture shape and magnitude of suppression

Summary

π^0 production measured in pp, pO and OO collisions

R_{OO}

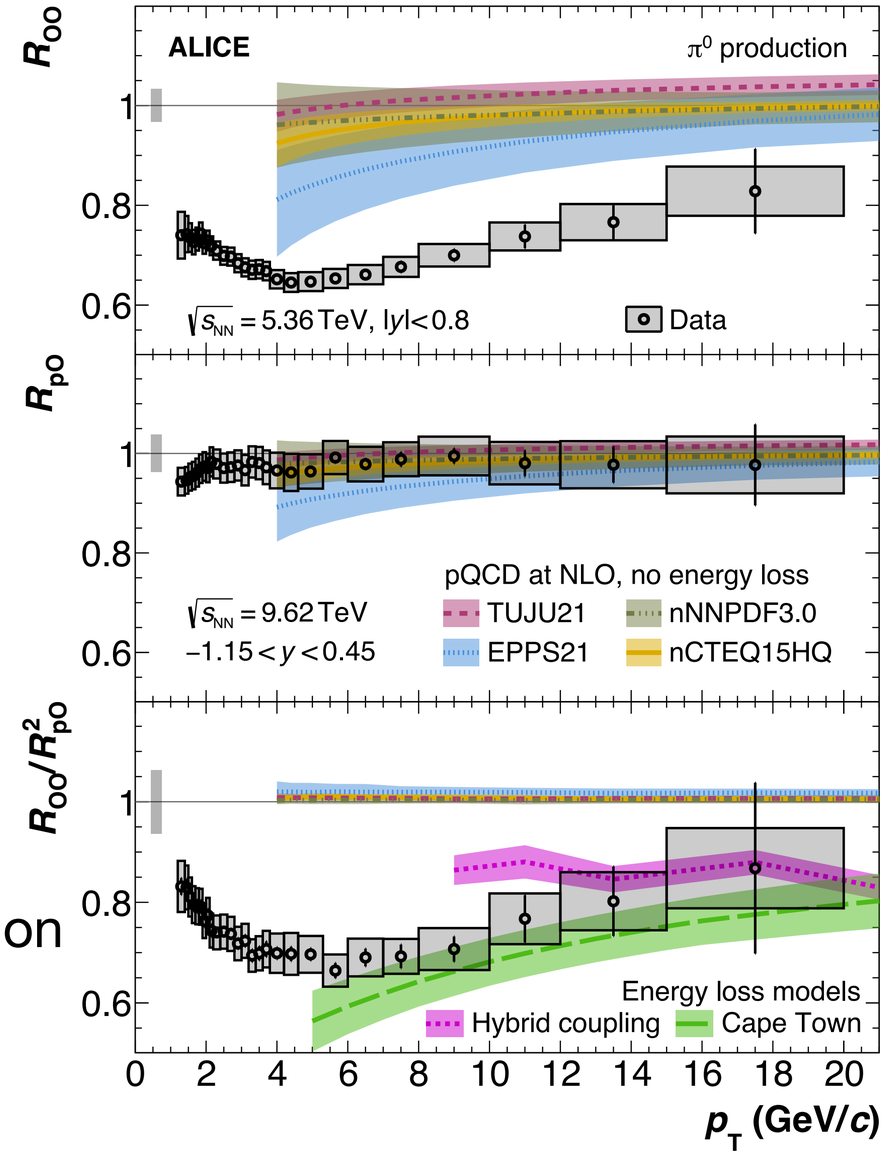
- **9σ** from unity, **1.8σ** from model without energy loss
- Shape similar to modifications in larger systems

R_{pO}

- Compatible with unity at intermediate p_T
- **First constraints on CNM effects in oxygen**

R_{OO}/R_{pO}^2

- Cancels CNM effects, **isolates energy loss** effects
- Data significantly suppressed w.r.t. all nPDFs
- Energy loss models describe shape and magnitude of suppression



Evidence for parton energy loss in OO: arXiv:2606.19967

Supplemental material: ALICE-PUBLIC-2026-002

Summary

π^0 production measured in pp, pO and OO collisions

R_{OO}

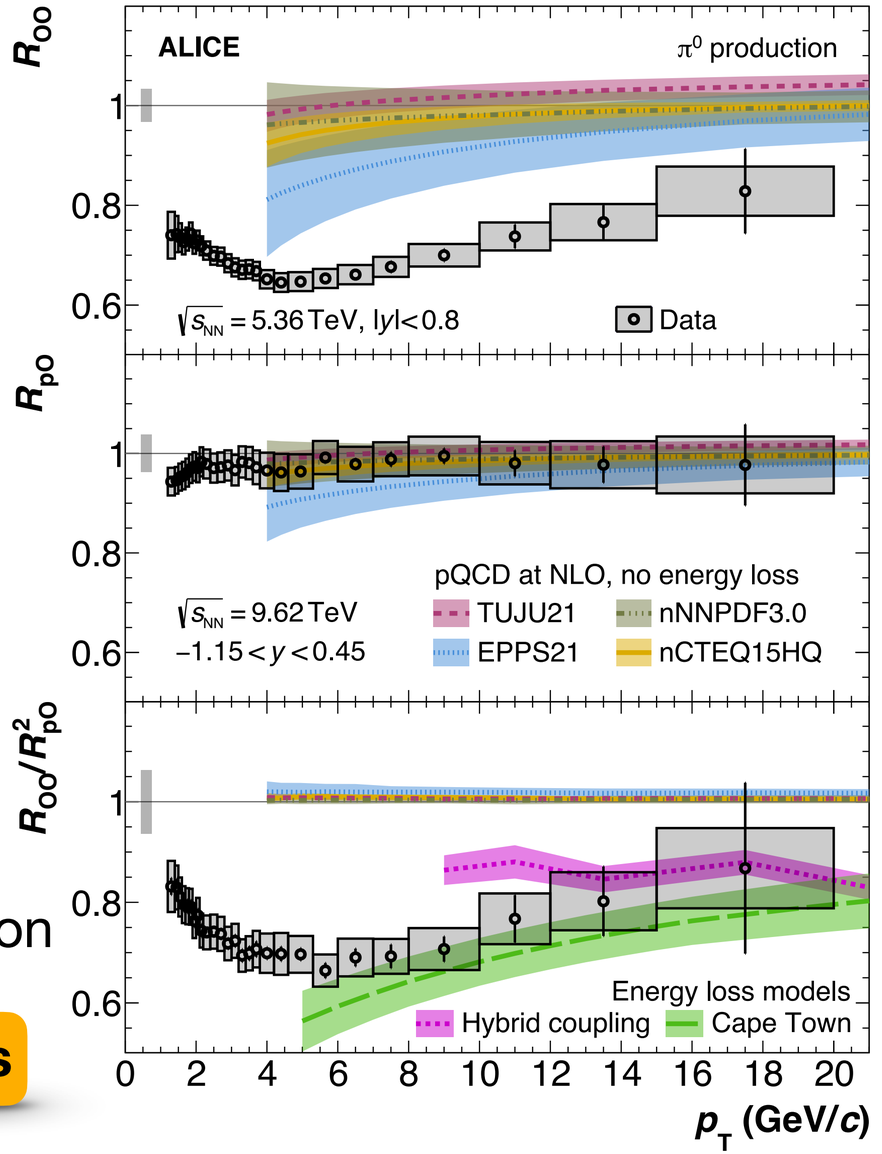
- **9σ** from unity, **1.8σ** from model without energy loss
- Shape similar to modifications in larger systems

R_{pO}

- Compatible with unity at intermediate p_T
- **First constraints on CNM effects in oxygen**

R_{OO}/R_{pO}^2

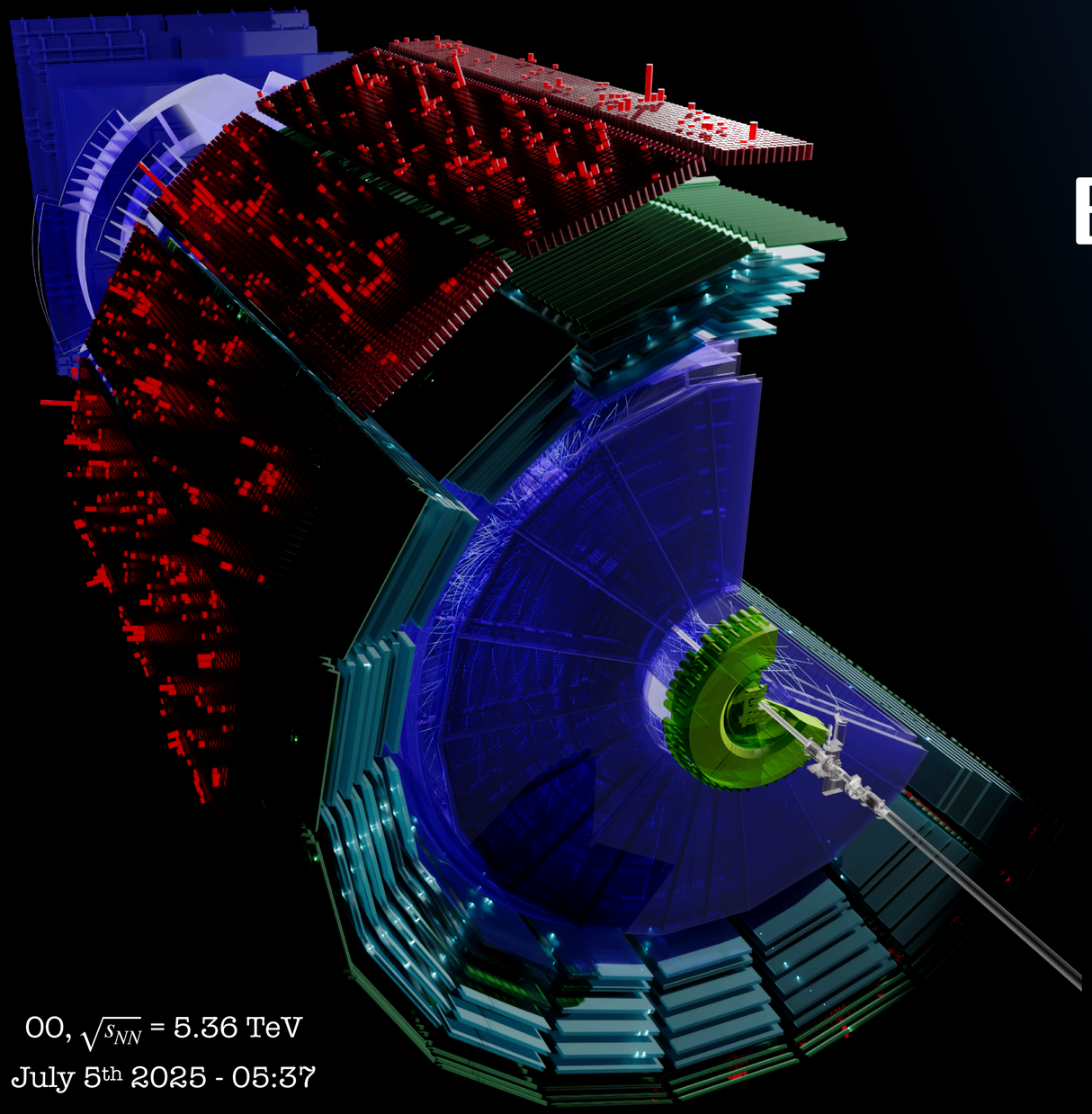
- Cancels CNM effects, **isolates energy loss** effects
- Data significantly suppressed w.r.t. all nPDFs
- Energy loss models describe shape and magnitude of suppression



➡ Strong evidence (4.9σ) for **parton energy loss in OO collisions**

Evidence for parton energy loss in OO: arXiv:2606.19967

Supplemental material: ALICE-PUBLIC-2026-002



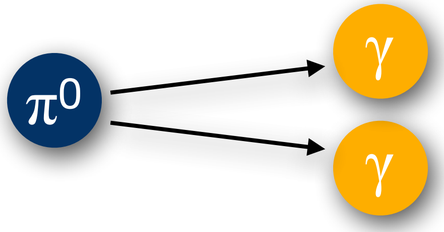
OO, $\sqrt{s_{NN}}$ = 5.36 TeV

July 5th 2025 - 05:37

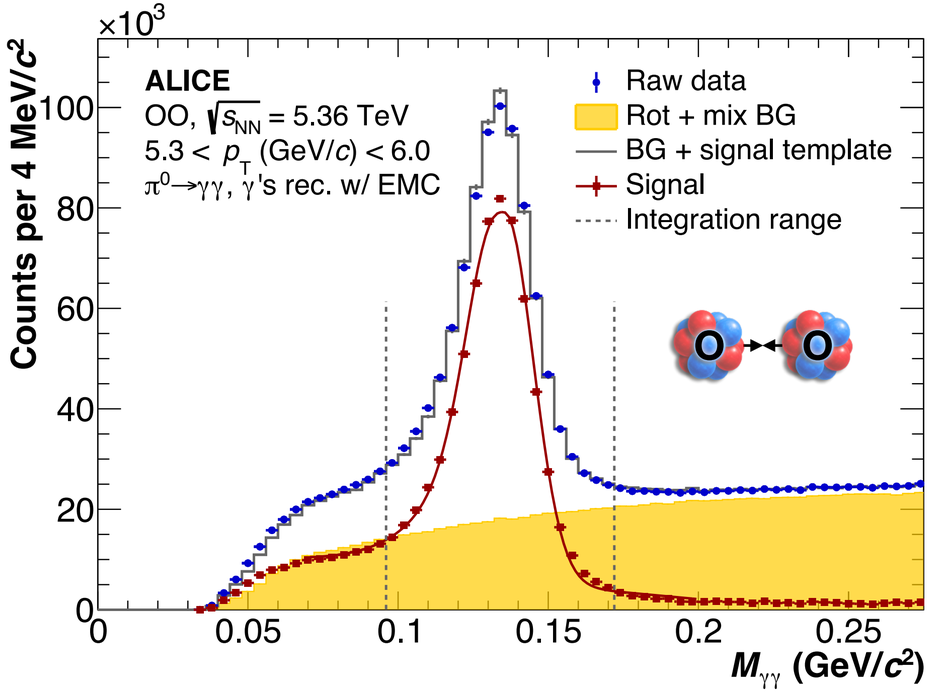
Backup

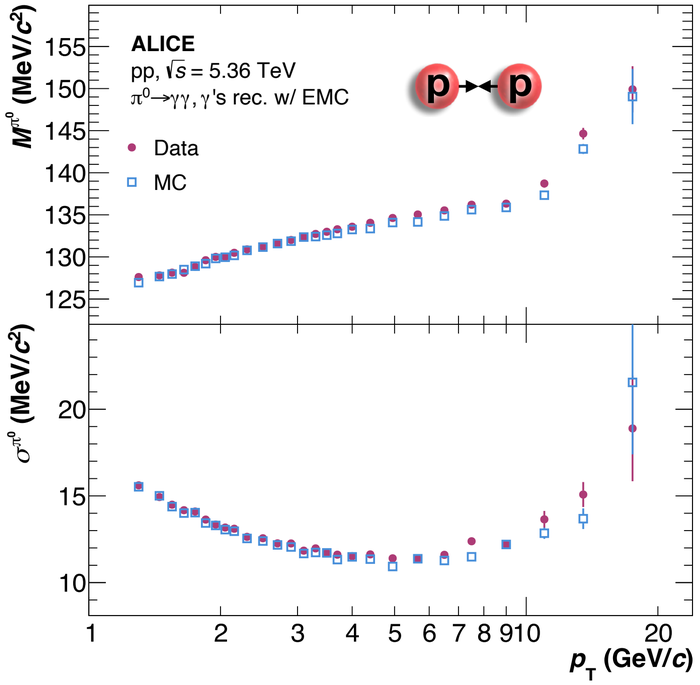
Reconstruction

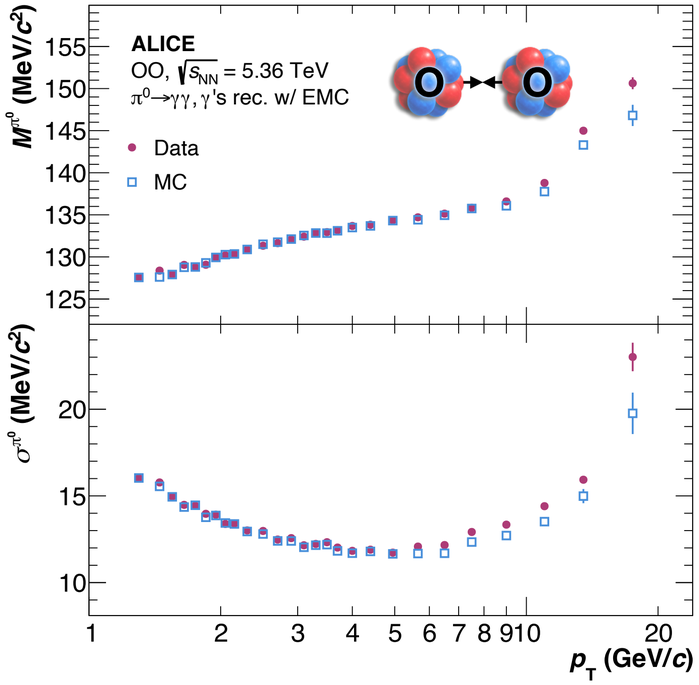
- Reconstruction of π^0 from their decay photons
- Background described via template of rotation and event mixing method
- Integral of signal peak
  → Raw yield
- Signal parametrization
  → Mass and width of π^0



$$M_{\gamma\gamma} = \sqrt{2E_{\gamma_1}E_{\gamma_2}(1-\cos(\theta))}$$







- Properties well described by Monte-Carlo simulation
- Measured mass and width similar in all systems

For description of rotation method, see JINST 18 (2023) P08007

Measured Cross Sections

π^0 production cross sections measured in

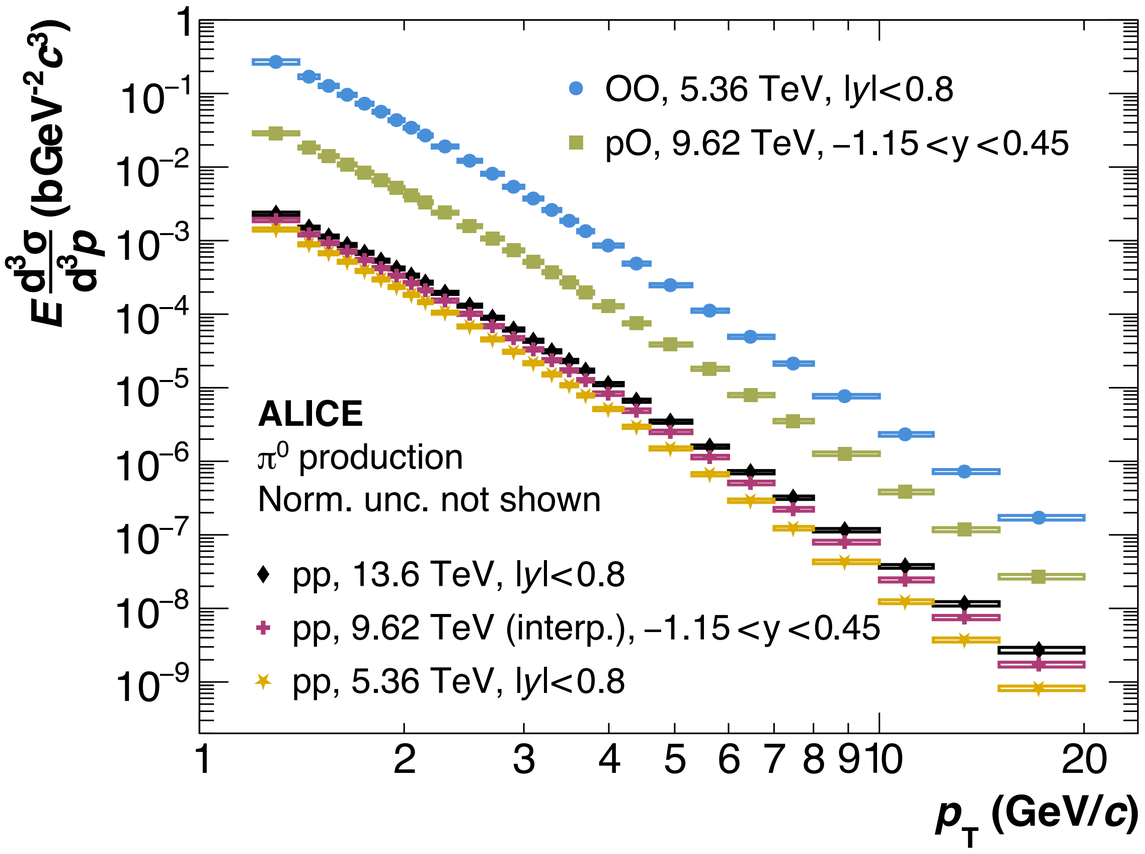
- **OO** (5.36 TeV), **pO** (9.62 TeV), **pp** (13.6 TeV) and **pp** (5.36 TeV)
- 1.2 GeV/c < p_T < 20 GeV/c, $|y_{lab}| < 0.8$
- Statistical uncertainty $\lesssim$ 1% at intermediate p_T
- Systematic uncertainty ~6%
  (4.2% from material budget → cancels in ratios)

Interpolation to pp, 9.62 TeV

1. Scale 5.36 TeV cross section up to 9.62 TeV
2. Scale 13.6 TeV cross section down to 9.62 TeV
3. Average the two cross sections
4. Repeat procedure with DNN and pQCD
   → Systematic uncertainty
5. Apply rapidity shift based on PYTHIA8

Normalization uncertainties

OO, 5.36 TeV: 2%
pO, 9.62 TeV: 2.7%
pp, 13.6 TeV: 2.6%
pp, 9.62 TeV: 2.6%
pp, 5.36 TeV: 2.6%

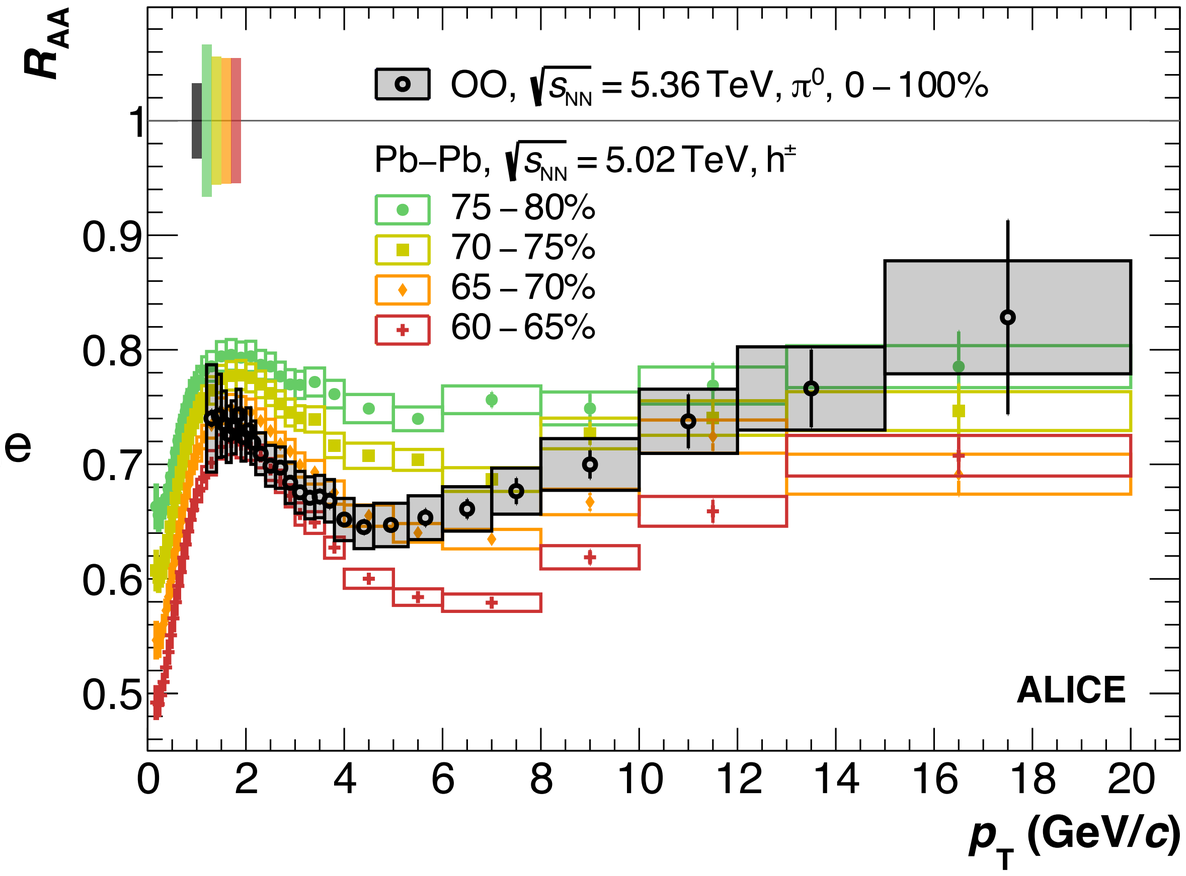


Connecting R_{OO} and R_{PbPb}

OO in comparison to different Pb—Pb centralities

$$R_{AA} = \frac{Y_{AA}}{\langle T_{AA} \rangle \sigma_{pp}}$$

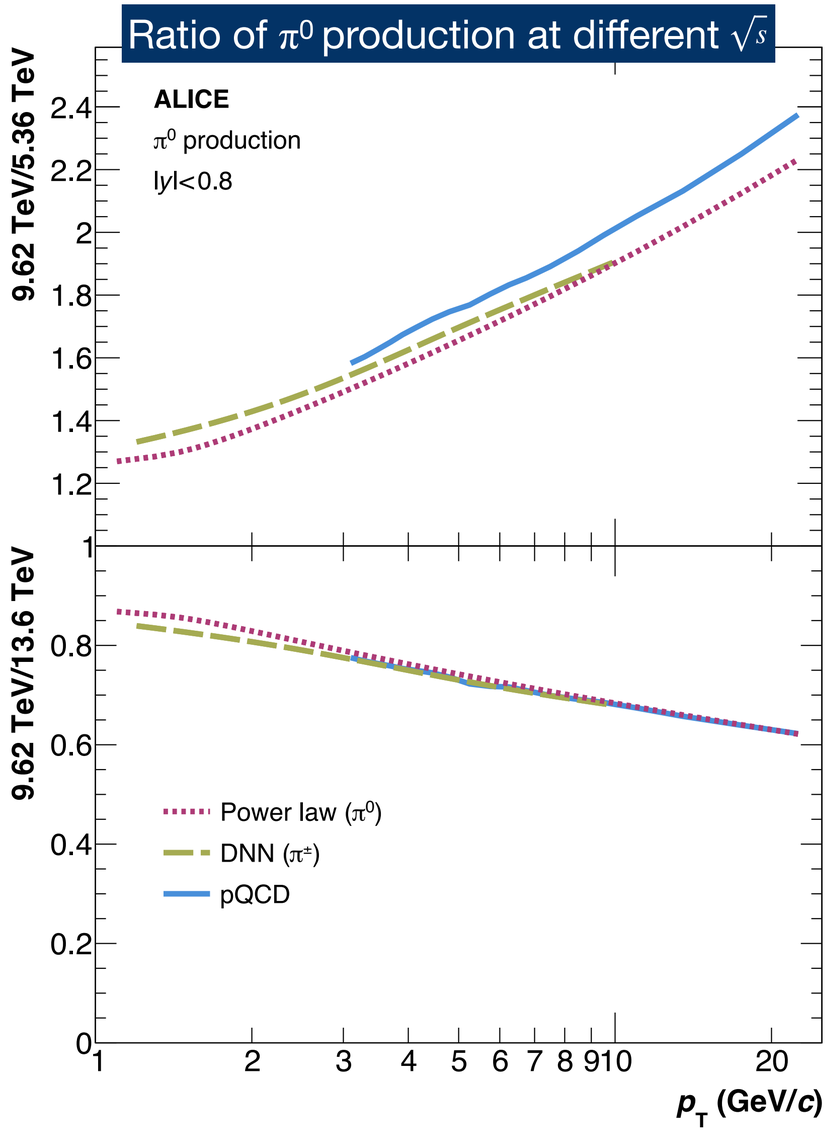
- OO 0-100%: $dN_{ch}/d\eta = 39$, $N_{coll} = 12.8$
- Corresponds to 75-80% Pb—Pb
  → Significant selection bias
- R_{OO} found to be very similar to 65-70% R_{PbPb}
- $dN_{ch}/d\eta$ distribution matters, not just the average
  → R_{OO} dominated by high multiplicities that are cut away in 75-80% Pb—Pb



Energy Dependence of π^0 Production

Three independent energy dependence estimators

1. Power-law parametrizations of π^0 cross sections
   - 2.76 TeV: ALICE, Eur. Phys. J. C 74 (2014)
   - 7 TeV: ALICE, Phys. Lett. B 717 (2012) 162–172
   - 8 TeV: ALICE, Eur. Phys. J. C 78 (2018) 263
   - 13 TeV: ALICE, JHEP 08 (2025) 035
2. Deep Neural Net trained on charged hadron production
   - DNN: M. Calmon-Behling et al., arXiv:2605.12490
3. pQCD calculations at NLO
   - pQCD: F. Jonas et al., arXiv:2602.15928

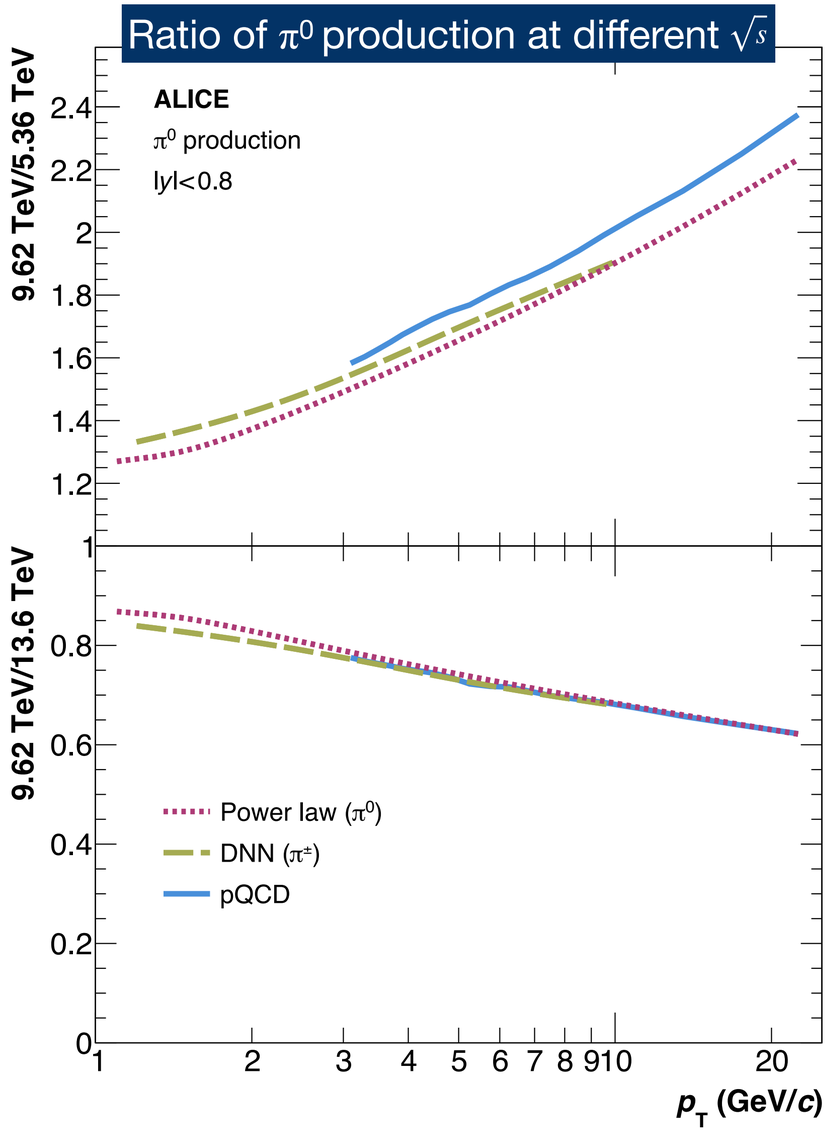


Energy Dependence of π^0 Production

Three independent energy dependence estimators

1. Power-law parametrizations of π^0 cross sections
   - 2.76 TeV: ALICE, Eur. Phys. J. C 74 (2014)
   - 7 TeV: ALICE, Phys. Lett. B 717 (2012) 162–172
   - 8 TeV: ALICE, Eur. Phys. J. C 78 (2018) 263
   - 13 TeV: ALICE, JHEP 08 (2025) 035
2. Deep Neural Net trained on charged hadron production
   - DNN: M. Calmon-Behling et al., arXiv:2605.12490
3. pQCD calculations at NLO
   - pQCD: F. Jonas et al., arXiv:2602.15928

➡ 3 independent methods
3 independent inputs

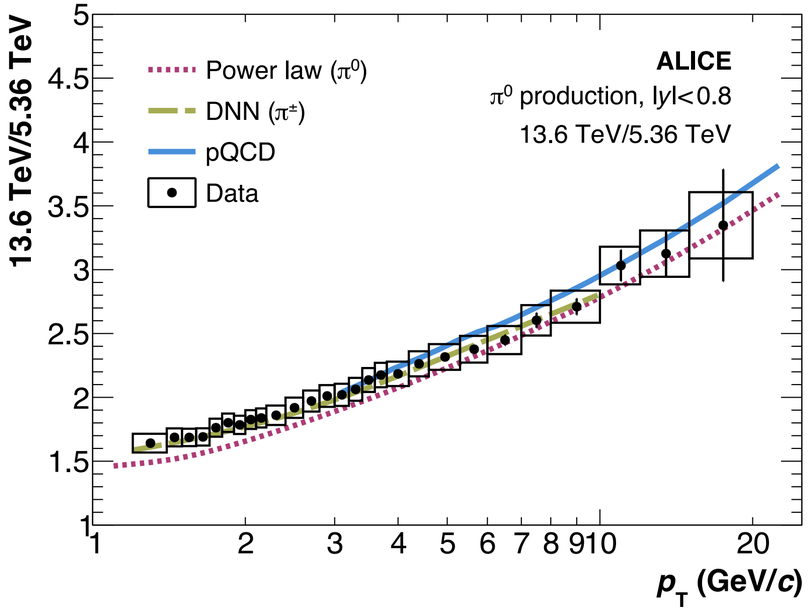


Energy Dependence of π^0 Production

Three independent energy dependence estimators

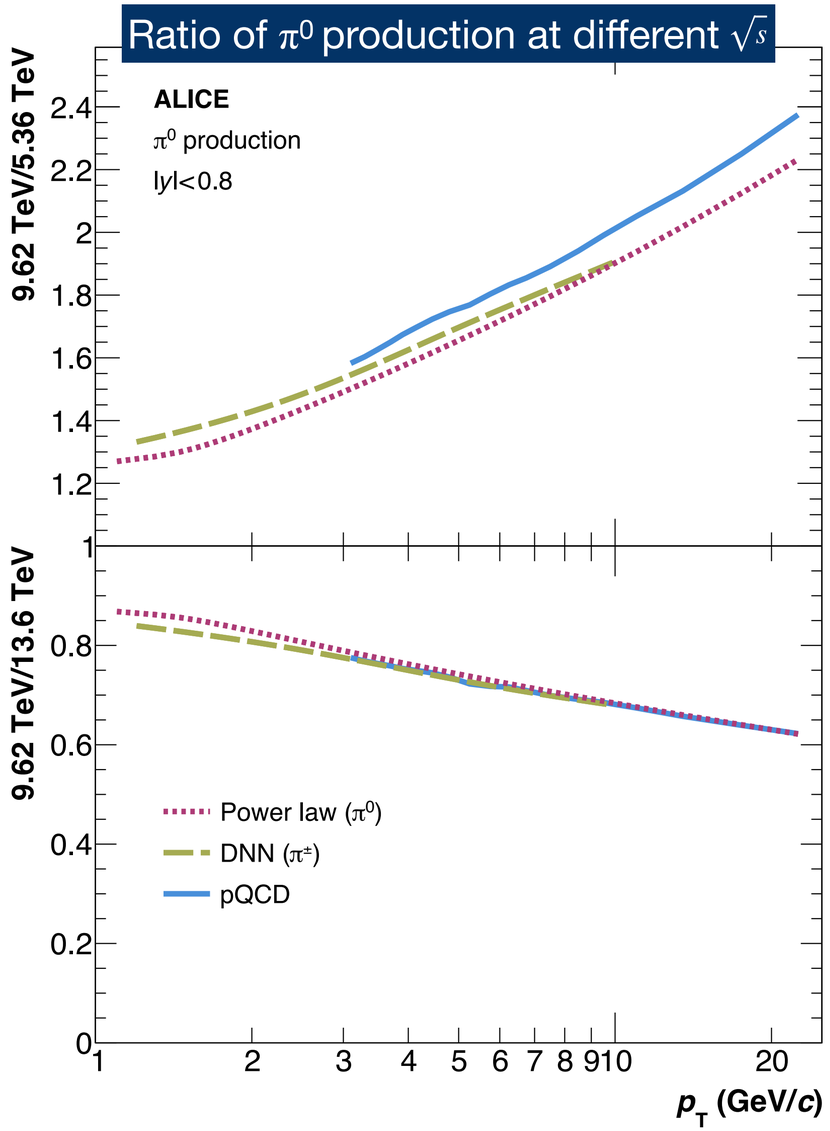
1. Power-law parametrizations of π^0 cross sections
   - 2.76 TeV: ALICE, Eur. Phys. J. C 74 (2014)
   - 7 TeV: ALICE, Phys. Lett. B 717 (2012) 162–172
   - 8 TeV: ALICE, Eur. Phys. J. C 78 (2018) 263
   - 13 TeV: ALICE, JHEP 08 (2025) 035
2. Deep Neural Net trained on charged hadron production
   - DNN: M. Calmon-Behling et al., arXiv:2605.12490
3. pQCD calculations at NLO
   - pQCD: F. Jonas et al., arXiv:2602.15928

➡ 3 independent methods
3 independent inputs



Validation

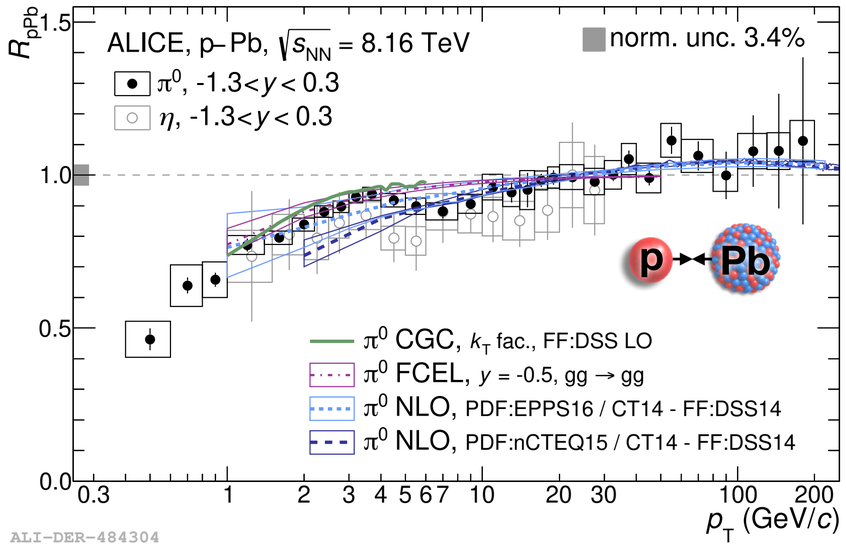
- 13.6 and 5.36 TeV measured
- All estimators compatible with measured $\sqrt{s}$ dependence
- Power law used as default (covers full p_T range)
- DNN and pQCD to determine systematic uncertainty



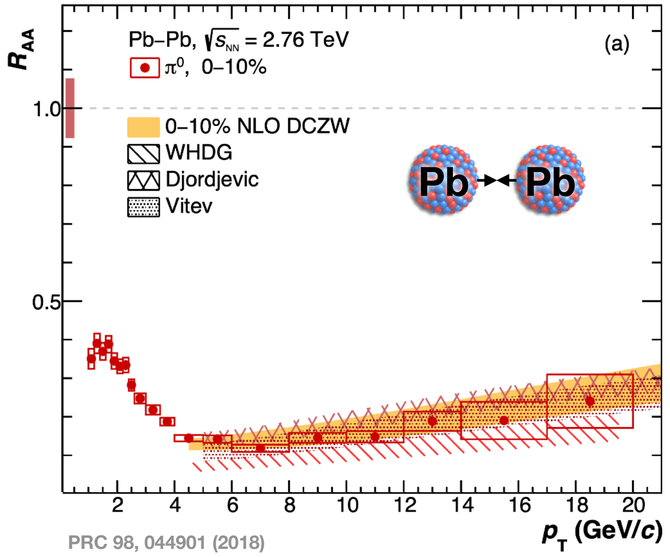
π^0's as the Ideal Probe

- Measured in many systems and energies in ALICE throughout the three LHC runs
- $B(\pi^0 \rightarrow \gamma\gamma) = 98.8\%$
  $\rightarrow$ Wide p_T coverage via ALICE's photon reconstruction methods
- Sensitive to parton energy loss in the QGP

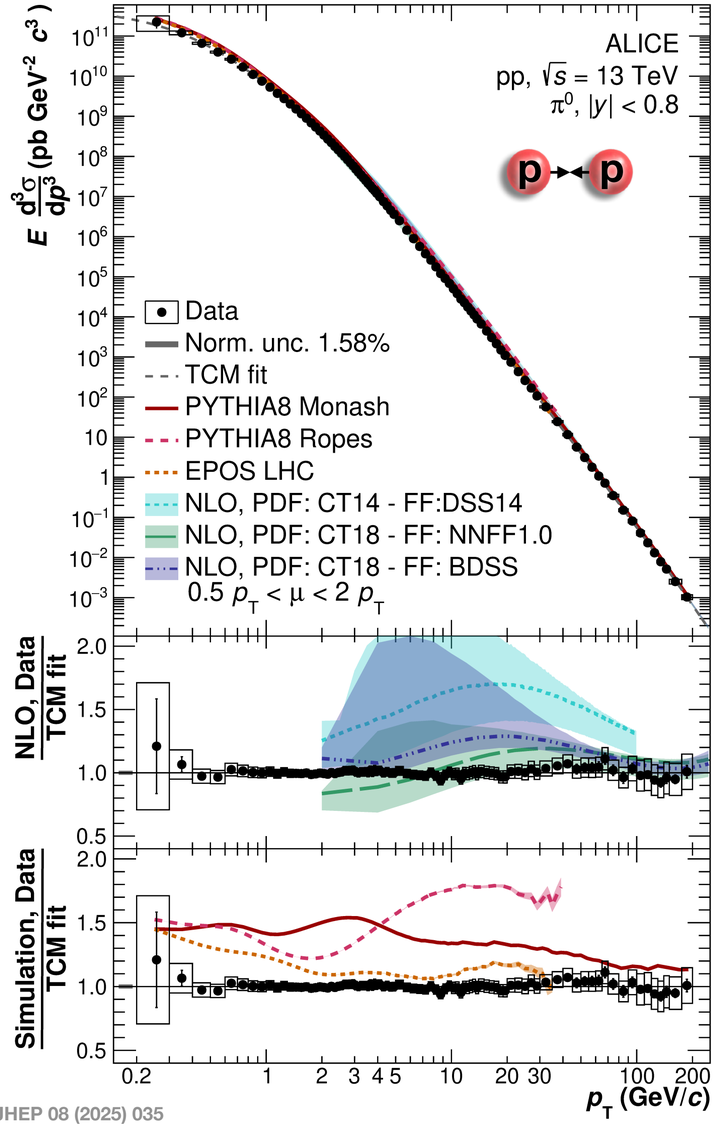
$\rightarrow$ π^0 as abundant and well understood **standard candle**



ALI-DER-484304



PRC 98, 044901 (2018)

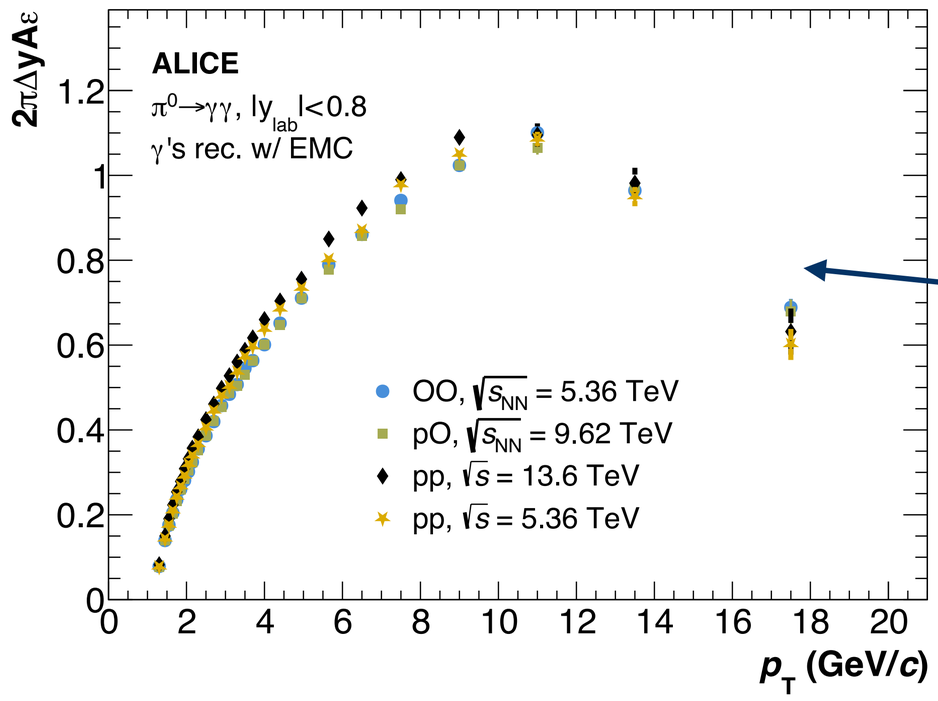


JHEP 08 (2025) 035

Corrections

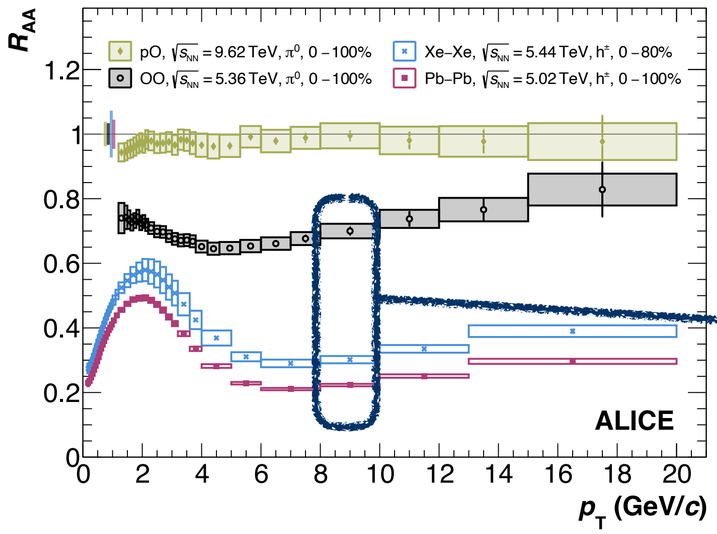
π^0 production cross section

$$E\frac{\mathrm{d}^3\sigma^{\pi^0}}{\mathrm{d}p^3} = \frac{N^{\pi^0}}{N_{\mathrm{evt}}}(1-S)\frac{1}{A\varepsilon_{\mathrm{rec}}2\pi\Delta y}\frac{1}{p_{\mathrm{T}}\Delta p_{\mathrm{T}}}\frac{1}{B}\zeta_{SL}\times\sigma_{\mathrm{vis}}$$

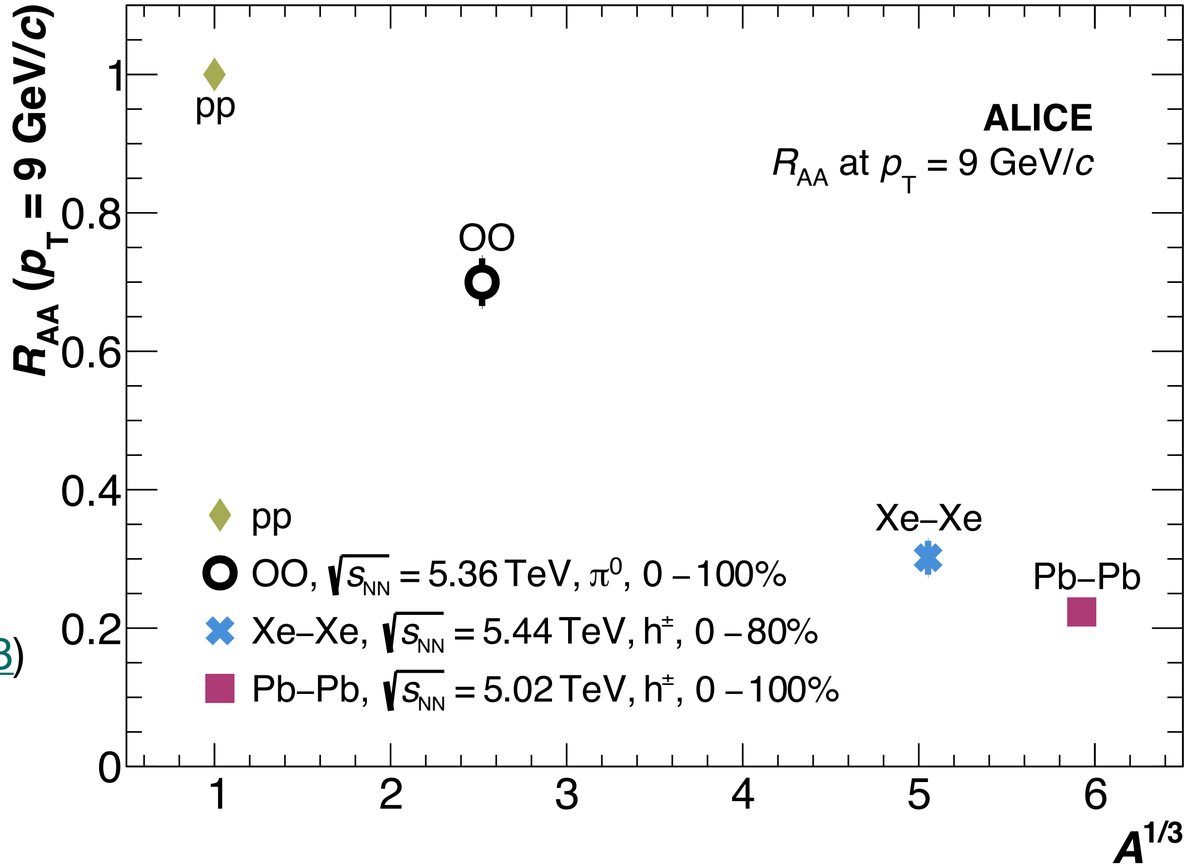


- N_{evt}: Number of collisions
  OO: 2.1 Billion, pp: 1.4 Billion
  (5% correction for pile-up)
- S: Secondary fraction (~4%)
- $A\varepsilon$: Detector acceptance and efficiency
- B: Branching ratio $B(\pi^0\to\gamma\gamma)$ = 98.8%
- ζ_{SL}: Signal loss (~2%)
- σ_{vis}: Visible cross section

System Size Dependence of the Suppression



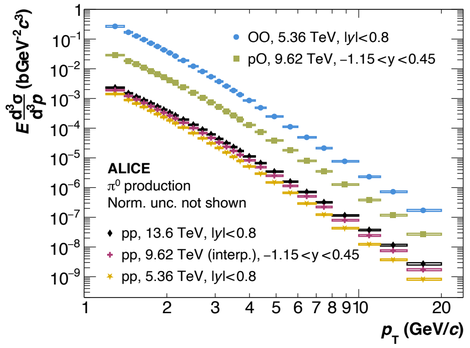
$$R_{AA} = \frac{Y_{AA}}{\langle T_{AA} \rangle \sigma_{pp}}$$

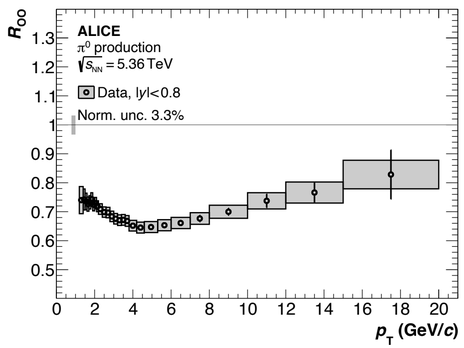


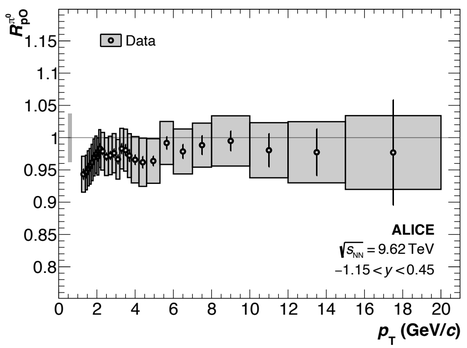
- System size dependence consistent with **suppression ∝ $A^{1/3}$**
- Suggests energy loss to scale linear with path-length of parton through the medium (e.g. F. Arleo and G. Falmagne, Phys. Rev. D 109, L051503)
- Interpret with caution! (neglecting CNM, convoluting collisional + radiative energy loss, $A^{1/3} \neq$ path-length, …)

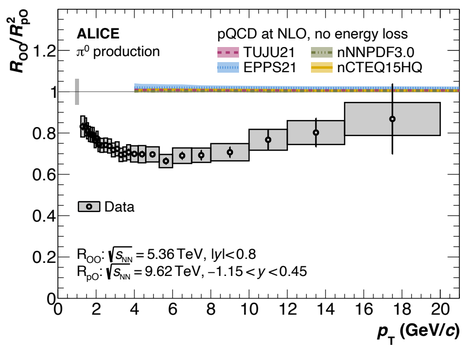
Relative Uncertainties

	Cross Section	R_{OO}	R_{pO}	R_{OO}/R_{pO}^2
Statistical	~1%	~1.5%	~1.5%	~2%
Systematic	~6% 4.2% (mat. budget) 2% (energy calib.) 2% (interpolation)	~3% ~2.5% (energy calib.) ~1.5% (signal extr.)	~3% ~2.5% (energy calib.) ~2% (interpolation) ~1.5% (signal extr.)	~5% ~4% (interpolation) ~2% (energy calib.) ~1.5% (signal extr.)
Normalization	2%, 2.7%, 2.6%, 2.6%, 2.6%	3.3%	3.7%	6.3%





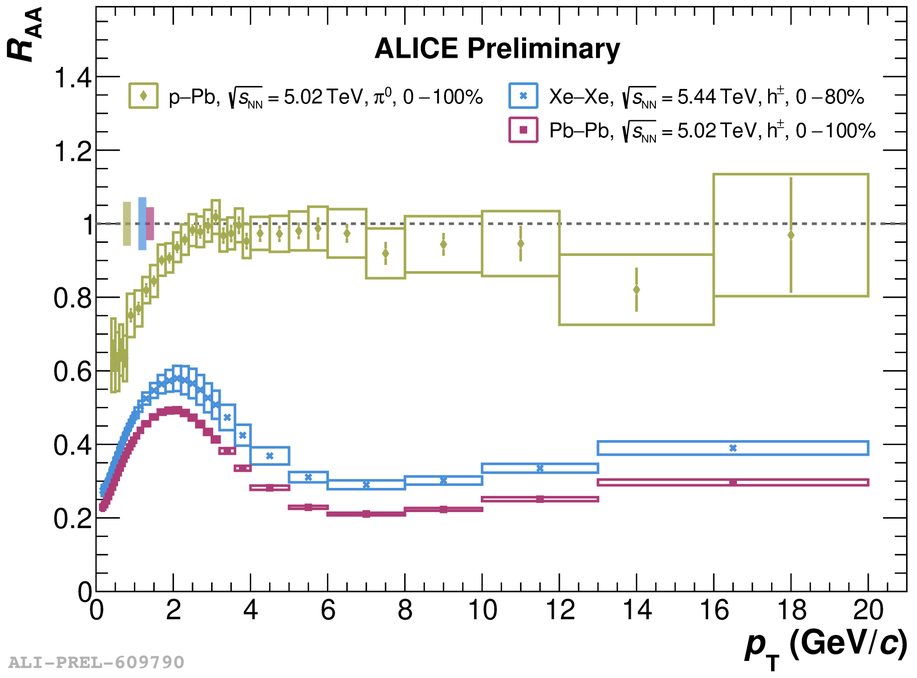




Nuclear Modification Factor in OO

- Nuclear modification factor (R_{AA}) of hadrons measured by ALICE in all available systems
  → p—Pb, Xe—Xe and Pb—Pb
- R_{AA} shows **strong suppression** (energy loss) **in Pb—Pb** and Xe—Xe
- **No suppression** found **in p—Pb** at high p_T

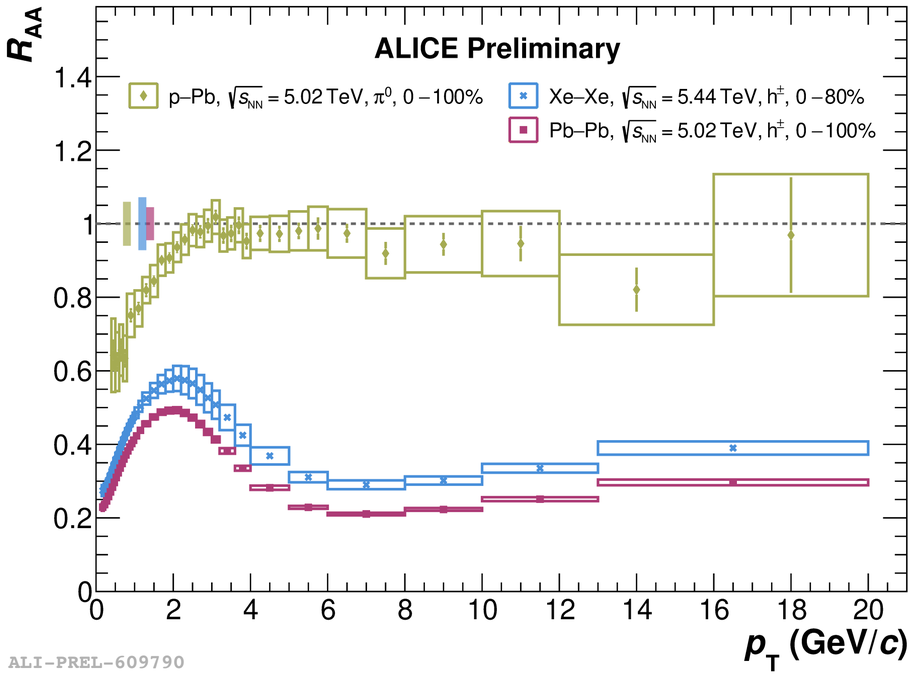
$$R_{AA} = \frac{Y_{AA}}{\langle T_{AA} \rangle \sigma_{pp}}$$



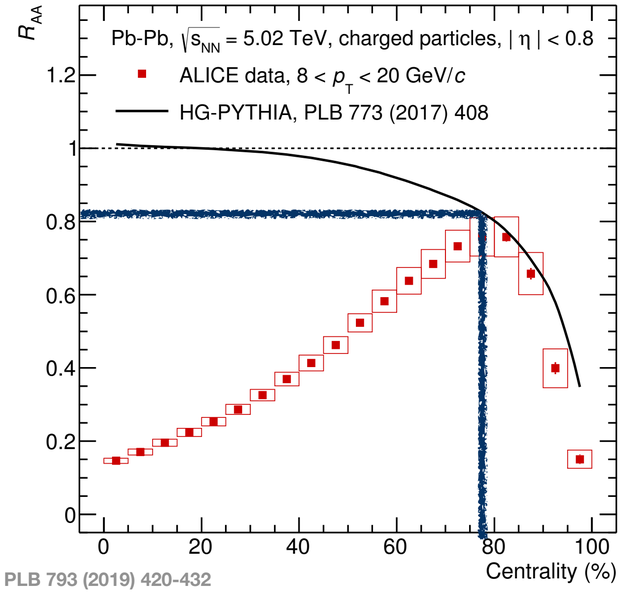
Nuclear Modification Factor in OO

- Nuclear modification factor (R_{AA}) of hadrons measured by ALICE in all available systems → p—Pb, Xe—Xe and Pb—Pb
- R_{AA} shows **strong suppression** (energy loss) **in Pb—Pb** and Xe—Xe
- **No suppression** found **in p—Pb** at high p_T

$$R_{AA} = \frac{Y_{AA}}{\langle T_{AA} \rangle \sigma_{pp}}$$



OO: A bridge between p—Pb and Pb—Pb



- Topology of OO collisions ($dN_{ch}/d\eta \approx 39$, $N_{coll} \approx 12.8$) similar to centralities of
  - 0-10% in p—Pb
  - 75-80% in Pb—Pb
- Both are affected by large selection biases

→ 0-100% OO collisions to probe this system size in a clean way!